Title
Research on Tubular Connections in Structural Work

Author
Bouwkamp, Jack

Publication Date
1960-12-01

To Prof. R.E. Davis, with the compliments of Jack Bouwkamp

SERIES 100
ISSUE 9

STRUCTURES AND MATERIALS RESEARCH
DEPARTMENT OF CIVIL ENGINEERING

RESEARCH ON TUBULAR CONNECTIONS IN STRUCTURAL WORK

BY
J. G. BOUWKAMP

REPORT TO
STANDARD OIL COMPANY OF CALIFORNIA AND
SHELL DEVELOPMENT COMPANY

DECEMBER 1960

INSTITUTE OF ENGINEERING RESEARCH
UNIVERSITY OF CALIFORNIA
BERKELEY CALIFORNIA

Structures and Materials Research

Department of Civil Engineering

RESEARCH ON TUBULAR CONNECTIONS IN STRUCTURAL WORK

by

J. G. Bouwkamp
Assistant Professor of Civil Engineering

Report to
Standard Oil Company of California
and
Shell Development Company

Institute of Engineering Research
University of California
Berkeley, California

December 1960

CONTENTS

RESEARCH ON TUBULAR CONNECTIONS IN STRUCTURAL WORK.

I. Abstract

This report discusses the test results of three welded structural joints of a two-dimensional truss built from steel tubes. The three connections were designed with different joint-eccentricities between the resultant of the web-member forces and the axial chord-member force. Also the results of tensile tests on four single tubes with welded transverse joints are reported herein.

The joints--each made up of a chord member, a vertical web member, and a 45°-diagonal web member--were placed in a specially designed loading frame. A direct tensile force was applied to the diagonal member by means of a 400,000-lb. hydraulic testing machine. Under this loading condition, the strains from about 60 strain gages were read for each of these specimens. Also the crack patterns of the stress coat applied to these joints were studied for information on the stress trajectories.

The tensile test results on the single tubes gave information about the weld and tube strength.

Some interesting conclusions were derived regarding the effect of joint eccentricity on the ultimate failure load for the type of joint tested.

II. Introduction

The application of tubes for structural work has increased rapidly over the last two decades. The early development in Germany has been followed by an increasing use of tubes in structural work, particularly in Germany as well as in Italy, France, and England. In the USA the application of welded tubular structures has been mostly limited to off-shore well-drilling structures and radar antennae. Reasons for this slower development in the USA are the small selection of available tube sizes and the resulting handicap on efficient structural design, and the great amount of labor required for the preparation of tubular joints for welding. The first disadvantage could be reduced if the selection of tube sizes--governed by the tube diameter as well as wall thickness--could be based on strictly structural considerations. This would give the structural designer a better choice than is possible now with the available sections, which are basically designed for other than structural purposes (e.g. line pipe). The second disadvantage can be reduced considerably by using the latest fully automatic tube-cutting machines.

Three important developments in Germany have greatly contributed to the increasing use of structural tubes: first, the wide variety of available tube sections for purely structural purposes; second, the extensive materials research, concentrated not only on the weldability but also particularly on the post-welding ductility of the steels used for the fabrication of these tubes; and third, the development of an automatic oxy-acetylene tube-cutting machine for cuts fitting flat as well as cylindrical surfaces (tubes). This machine operates fully automatic after the required cut-shape has been preset by a simple three-lever operating system. The lever settings are governed by the three variables describing the cut, namely: the inner diameter of the tube to be cut, the outer diameter of the tube to which the cut tube has to be welded, and the angle between the two tube axes. A simultaneous rotation of the concentrically clamped tube and a combined linear and angular movement of the cutter results in an excellent clean cut. No further manual trimming or adjustment is necessary, since the preset cut is mathematically correct and has immediately the correct cutting angle and beveled edge required for an immediate subsequent welding operation (see Fig. 1). This machine not only reduces the old-fashioned manual cutting operation time to only 10%, but also leads to 30% savings in the welder's time and electrodes, due to the great accuracy of the cut. For example, setting, mounting, and cutting of an 8-in. inside-diameter tube with 1/4-in. wall thickness, making a 45^{o} angle with a 13-in. outer-diameter tube, takes only 6 1/2 minutes of which only 3 minutes are actual cutting time. The fabrication cost is further lowered by using two cutting machines simultaneously at both ends of the tube, thus reducing the operation time even more.

Besides the discussed developments which can definitely lead to a greater application of tubes in structural work in the USA, it is further necessary to obtain a better insight into the actual behavior of welded joints. This will lead to a more rational joint design and result in further savings which will make tubular structural work economically more advantageous.

One of the great advantages of tubes in general is the flexibility of the tube wall, which always allows a redistribution of stresses in the welded joints. This favorable effect may partly or completely disappear if gusset plates are used to transfer the loads. These gusset plates will normally cause high stress concentrations in the tube wall right where the gusset plate starts to transfer the load. The only way to prevent this stress concentration is to design the gusset plate with a considerably reduced stiffness at that particular location. By increasing the stiffness from that point towards the center of the connection, a gradual load transfer between tube wall and gusset plate will be achieved. Under these circumstances the design of gusset plates in tubular work should be handled with great care, since the joint rigidity will greatly affect the stress distribution and the failure load.

Since most welded tubular joints are designed without gusset plates, the research reported herein has been restricted to directly welded tubes. Although the effect of the diameter-ratio of connected tubes, the effect of the diameter-to-wall-thickness-ratio, and the effect of outer stiffening rings or inner concrete fillings are also of great significance for the ultimate failure load, the tests described herein deal with an investigation of the important joint-eccentricity effect of the web-member and chord-member-forces. Figure 2 shows a typical tubular truss in which the tube center lines follow the truss system lines exactly. Figure 3, however, indicates the possible "positive" and "negative" joint-eccentricities. These different eccentricities will result in different connections. For instance the positive eccentricity will in many cases result in a joint in which the web-members are not interconnected. The generated weld-length of this connection depends on the diameter-ratio of the connected tubes, the angle between their axes, and the amount of eccentricity. Nevertheless, in general the situation will be quite different for a negative-eccentricity joint. In that case a considerable interconnection between the web members will occur and will result in an immediate transfer of the vertical component of the diagonal-member force into the vertical compression member. This reduces the load transfer from the diagonal to the vertical web-member via the wall of the chord-member tube. The improved load-transfer will, of course, affect the ultimate load in the tensile diagonal member since the joint response will be different depending on the joint eccentricity. That the load transfer will be improved can also be illustrated by the fact that the tensile member is welded to the chord member completely and the compression member is cut to fit over the tension member. This arrangement will cause the compression member to push the tension member against the chord tube and thus reduce the tensile load in the tension-member welds.

The cost of fabrication for a negative-eccentricity joint will, of course, be more than that for a positive-eccentricity joint, since extra cutting of the vertical compression web-member is necessary to fit the diagonal member. Also the subsequent welding will be more expensive.

The relative effect of joint eccentricity becomes very important if the failure load of the joint is compared with the ultimate strength of the diagonal tension-member. It will be shown to what extent the joint eccentricity affects the developed strength of the joint itself relative to the ultimate strength of the member. If it is necessary to over-design a member in tension to meet the required strength in the connection as based upon the design loads, then the advantage of the light tubular structure will be lost. However, if it is possible--by changing the joint eccentricity--to design a joint connection of equal or greater strength than the connecting member itself, a further optimization of tubular structures with loaded tension members will be achieved.

III. Test Specimens

a. Single-tube test specimens. Two types of single-tube test specimens were designed to provide information on the weld strength under tension (see Fig. 4). These tubes were identical to the diagonal web-members of the joint specimens, which members were subjected to tension. The tubes--actually line pipes--were electric resistance-weld pipes, grade B, manufactured in conformance with API specification 5L, which is similar to ASTM A135-58T. The outside diameter was 6 5/8 in. and the wall thickness 3/16 in. Each specimen was made from two pipes, each 4 ft. long, welded together. One type was butt-welded with a Lincoln Fleetwood No. 35 electrode under a 25 volts and 100 amperes. This electrode meets the A.W.S. Specification E6011. The other type of specimen had a concentric steel ring 1 1/2-in. thick, to which the two 4-ft. lengths of pipe were fillet-welded. Fleetwood No. 35 electrode was also used for these 5/16-in. fillet welds. The voltage and amperage were identical to those used for the butt-welding operation. Since it was only necessary in this program to obtain a direct comparison between the failure loads of the single-tube specimens and the joint specimens, no specific tests were designed to test the operator's welding ability. To obtain a basis of comparison, however, it was specified in this program that the same operator should make all the welds in both the single-tube specimens and the joint specimens, and that none of the welds should be stress-relieved.

The German specification DIN 4115 for tubular structural work requires certain tests to prove the welding ability of the operator. One of these DIN-tests, in which two tubes are connected by a full fillet weld at each end of a short tube, the inner diameter of which fits precisely around the ends of the two main tubes, could not have been performed since no standard pipe sections are available in the USA to design such a connection.

<u>b. Joint test specimens.</u> These specimens were designed with different eccentricities between the resultant web-member forces and the axial chord-member force. The eccentricities were designated as positive, zero, and negative, see Figures 5, 6, and 7. For a zero-eccentricity joint, all member system lines pass through one point. A positive-eccentricity joint has a resultant web-member force which lies outside the chord-member system-line of the truss (see Fig. 3). A negative-eccentricity joint causes a resultant web-member force inside the chord-member system line, as shown in the same figure. These resultant forces produce a secondary couple

causing additional stresses in the wall of the chord-member tube, namely, tensile stresses in the tube wall next to the web members if the joint eccentricity is positive, and compressive stresses if the joint eccentricity is negative.

The three joint specimens were designed to fit a specially designed loading frame with an allowable load capacity of 600,000 lb. (see Fig. 8). This frame, while resting on the upper head of a 400,000-lb. testing machine, supported both the vertical web member and the chord member of the joint. The diagonal web member--in a vertical position during the test--was attached to the lower head of the testing machine and was subjected to a tensile load.

Since the eccentricity effect was to be investigated by only three specimens, an extreme value for the positive and negative eccentricities was chosen. These eccentricities were equal to 3 3/16 in., or 1/4 of the outside diameter of the chord-member tube (O. D. = 12 3/4 in. and wall thickness 1/4 in.). The compression web member in each specimen had an outside diameter of 6 5/8 in. and a wall thickness of 3/8 in. The diagonal web member in each specimen had the same outside diameter of 6 5/8 in. but a wall thickness of only 3/16 in. In all three joints the diagonal member--subjected to a tensile force--was welded completely to the main chord member, as indicated in Figure 9. All joint welds were made by the operator who welded the tensile specimens. Again a Lincoln Fleetwood No. 35 electrode was used under the same voltage conditions as for the simple tensile specimens. The amperage, however, was reduced for practical reasons to 100 amperes.

The compression web members for the zero and negative-eccentricity joints were welded to the diagonal and chord members, thus producing under load an additional compressive force to the earlier welds connecting the diagonal and chord member. The chord member and web member, which were under compression, were provided with a special stiffening arrangement to prevent local buckling of the tube walls near the thick supporting or loading plates. The angles--with reduced stiffnesses--were designed to obtain a gradual load transfer into the tube, without extreme restraint of the transverse expansion of the tube wall. Two steel plates were bent and welded to the diagonal tension member of each specimen to obtain a proper load transfer to this member.

The joints were completely unrestrained by any type of stiffening arrangement. The chord-member tube was open on the unloaded side.

IV. Test Preparation and Procedure

a. Single-tube test specimens. On each of these specimens at least 12 electric resistance-wire strain gages were used to investigate the stress distribution around the tube. These gages were placed in pairs 120° apart on either side of the weld. Since the relatively rigid ring of the fillet-weld type of specimen prevents a free contraction of the tube cross-section, additional bending moments acting in the longitudinal direction will be introduced in the tube wall. To trace this effect in one specimen (F-1), 16 more gages were mounted in pairs on one side of the weld along an axial line.

The butt-weld specimens, B-1 and B-2, and the fillet-weld specimens, F-1 and F-2, were all tested in a 4,000,000-lb. testing machine. These specimens were provided with a solid steel plug, 18 in. long, inserted at each end of the tube, to maintain the tubular shape under the action of the load-transferring grips of the testing machine.

b. Joint test specimens. The three joint test specimens were instrumented with strain gages and stress-coat to obtain a basic picture of the strain distribution and the stress flow. The stress-coat was used to evaluate qualitatively the stress pattern. Electric resistance-wire strain gages--approximately 60 on each specimen--were applied to measure the strains at some chosen stations and to determine the principal stress directions (see Figures 10, 11, and 12). Where necessary the gages were assembled in 0^{o}-45^{o}-90^{o} rosettes. The gages on the chord-member tubes were basically designed to evaluate the local stress directions. These results could then be checked against the stress-coat results. The gages on the web members were designed to obtain information about the strain and stress distribution in these members, close to the welded connections, where the load transfer could be expected to be greatly concentrated. As figures 10, 11, and 12 indicate, the gages were placed on mainly one side, except some single gages being placed at diametrically opposite locations. The stress-coat was only applied on the side other than that where the gages were placed. An exception was the positive-eccentricity joint, which was coated on both sides. Before applying the stress-coat on the specimens, first a coat of aluminum paint was sprayed on the tubes to allow for a better observation of the stress-coat cracks while under load.

The joint specimens were loaded in a specially designed loading frame 12 ft. high (see Figure 8). This frame could be mounted in a 400,000-lb. or a 4,000,000-lb. testing machine, depending on the expected failure load for the specimens. Since the failure loads for the joint specimens tested in this series were all expected to be less than 400 kips, the loading frame was mounted in the 400,000-lb. Baldwin testing machine. The 36 WF 150, 4 ft. 10 in. long top beam of the welded loading frame rested on the upper head of the testing machine. The two lower 24 WF 76, 7 ft. 6 in. long beams were coupled at each end of the top flanges by means of heavy bearing plates making a 45° angle with the beams. These beams--coupled at the bottom flanges also--were 24 1/2 in. center to center and were supported by four welded 10 by 1-in. straps, each welded to the top beam and spliced at mid-height. The 15-in. opening between the two 24 WF-beams could easily take the 6 5/8-in diagonal joint-tube. While the vertical web- and chord-member tubes were supported by spherical blocks, mounted on the inclined (45°) bearing plates in order to obtain the proper load direction in these members, the test load was applied to the diagonal web member, which was in a vertical position while being tested. The load was applied by the lower head of the testing machine, which held a vertical pin in a spherical supporting block. The other end of this pin was provided with a U-shaped cast-iron grip which held the horizontal pin passing through the legs of the grip and the reinforcing plates of the diagonal web member. Since both supports and the load-transferring pin were spherically shaped, it was possible to mount the specimen without introducing significant out-of-plane eccentricities in the applied load or the reactions. The direction of the test load P was brought into complete alignment with the axis of the diagonal web tube.

The bearing blocks for the compression members were centered with respect to the axis of the member.

V. Test Results

a. Single-tube test specimens. All four specimens were tested to failure. The two tubes which were butt-welded failed in the weld, (see Figure 13a). Both fillet-welded tubes, however, failed in the tube wall, (see Figure 13b). The following failure loads were recorded:

butt-welded:	B-1	failure load:	200 kips
	B-2	:	200 kips
fillet-welded:	F-1	failure load:	252 kips
	F-2	:	259 kips

The strain gages on the B-1 and B-2 specimens clearly indicated bending in the tube wall near the weld, caused by an incomplete penetration of this butt weld.

Using the actual weld area as measured after failure, the following average normal stresses in the weld were computed:

B-1 $\sigma_{average} = 52{,}400$ psi

B-2 $\sigma_{average} = 47{,}600$ psi

One should realize that the true failure stress was probably 40 to 50% greater than the computed stress. The eccentricity of the weld itself--as caused by the insufficient penetration--together with the fact that the failure must have started at the weakest point in the weld, presumably where the throat thickness of the weld was the least--justify this assumption.

The 5/16-in. fillet welds performed excellently. The theoretically high stress concentrations in the tube wall just next to these welds could not be traced by the strain gages, since the stresses were so localized and changed so rapidly. These stresses are caused by both the restrained radial contraction and the restrained end-rotation of the tube wall. Figure 13b shows clearly the type of failure and the associated tube-necking which occurred shortly before failure.

b. Joint test specimens. These specimens were also tested to failure, with results as follows:

Positive-Eccentricity Joint:	Failure load P = 137 kips	(50%)
Zero-Eccentricity Joint :	" " P = 209 kips	(75%)
Negative-Eccentricity Joint:	" " P = 277 kips	(100%)

The results clearly indicate the great effect of the joint eccentricity for the tested connections. A comparison of the failure loads for the positive-eccentricity joint--eccentricity 1/4 of the chord-tube diameter--and the negative-eccentricity joint--having the same but opposite eccentricity--shows a difference in load-carrying capacity for the first connection of 50%, as compared with the load carried by the negative-eccentricity joint. Similarly the load-carrying capacity of the zero-eccentricity joint was 25% less than the failure load for the negative-eccentricity joint.

An even more important comparison can be made by considering these failure loads as against the failure loads of 252 kips and 259 kips for the tubes of specimens F-1 and F-2. This comparison evaluates the capability of the tested joint connections to develop the same strength as the actual tension member. Using an average ultimate load of 255 kips for the single member, the following joint-strength factors were determined:

Positive Eccentricity	Joint-Strength factor	= 0.54
Zero Eccentricity	" " "	= 0.82
Negative Eccentricity	" " "	= 1.08

These factors would not be increased by applying heavier welds since all specimens failed in the tube walls (see Figure 14). For a close-up of the failure in the positive-eccentricity joint, see Figure 15. Based on these results, it is clear that for this particular joint arrangement the negative-eccentricity joint is superior to the others tested.

Observing the failure modes as given in Figure 14, it should be noted that the failure for the negative-eccentricity joint did not actually take place in the joint itself but about 1/2 in. away from the weld in the tube wall of the diagonal tension member. That this tube could fail under a load larger than the average obtained from the simple tensile tests must have resulted from the radial restraining effects on the tube by the joint connection at one end and the load-transferring plates at the other end. It is interesting to know that under the increasing load prior to failure the tubular cross-section of the diagonal tension member became elliptical. The 6 5/8-in. diameter increased to 7 in. perpendicular to the plane of the truss and decreased to 6 3/8 in. just beneath the weld connecting the two web members. This effect was also clearly indicated by the failure of the wall, as the wall above the crack was pulled inward compared with the tube wall below this crack.

The failure of the zero-eccentricity joint was caused by a crack in the diagonal-tube wall right at the toe of the weld, connecting the two web tubes (see Figure 14).

A crack in the wall of the chord tube at the toe of the weld connecting the diagonal to the chord member caused the failure of the positive-eccentricity joint. All three failures were caused by combined high transverse shear and normal stresses over the thickness of the tube wall.

Figure 16 gives the load-strain curves for 2 sets of gages on the compression web-member tubes of each joint, namely:

Pos.-Ecc. joint:	gages 1-2 and 5-6
Zero-Ecc. joint:	gages 1-2 and 13-12
Neg.-Ecc. joint:	gages 1-2 and 13-12

The first gage of each set indicates the axial gage while the second gage indicates the tangential gage at the particular location. The graphs of Figure 16 present the strains in microinches/in.--(10^{-6} in./in.)

--under an increasing load P in kips, as well as the elastic strains obtained by unloading and reloading the specimen. The No. 1-gage curves for all three specimens showed a positive strain in the compression member. This result indicated an eccentric load distribution in this web member next to the weld, and implied that the side of the vertical next to the diagonal must be highly stressed in compression. This was indeed confirmed by the strain readings for the gages at those locations (gages No. 5 and 13). These gages also revealed that for the same load the strains in the negative-eccentricity joint were smaller than the strains in the joint with a positive eccentricity. Tables I, II, and III present the total and elastic strains of each of these gages at different load levels. These tables also give the axial and tangential stresses as determined from these elastic strains at the particular locations.

The load-strain curves for two sets of gages on the tension diagonal web member of each specimen are given in Figure 17. The following sets of gages--representing respectively the axial and tangential gage--are considered:

Pos.-Ecc. joint: gages 13-12 and 17-18

Zero-Ecc. joint: gages 14-15 and 26-25

Neg.-Ecc joint: gages 14-15 and 26-25

The graphs of Figure 17 clearly show the high strain concentration for the gages located next to the vertical compression member. The strains measured at gage positions 17-18 and 26-25 are only a fraction of those measured at the positions 13-12 and 14-15. This overall result indicates the severe stress condition in the tube walls of the two web members at the point of first intersection. A comparison between the tensile strains of gages 14 for the zero- and negative-eccentricity joints clearly shows at the same load level the lower value of strain for the negative joint eccentricity. The total and elastic strains for each of the gages under observation, as well as their associated stresses, are presented in Tables I, II, and III.

From the results shown in Figures 16 and 17 and Tables I, II, and III, it can be concluded that the strains and stresses at the considered locations decrease if the web-member tubes are inter-welded over a greater length. This arrangement will then lead to a more uniform stress distribution over the tube wall and increase the ultimate failure load.

A final evaluation of the stress distribution in the vertical (compression) and diagonal (tension) web members is given in Tables IV, V, and VI. These tables represent the principal state of stress for each of the 3 joint specimens at different load levels. At these load levels the elastic strains were determined by unloading and reloading the specimens. Table IV indicates that the maximum tensile stress in the diagonal tube occurred at a location next to the weld (gages 12-13). Tables V and VI for the zero and negative eccentricities show clearly that the maximum stress in the diagonal or tension member did not appear next to the weld (gages 14-15), but rather farther along the weld. This is implied by the strains for gages 16-17-18 of the zero-eccentricity joint, and by gages 22-23-24 for the negative-eccentricity joint. The greater length of the weld between the web members caused the favorable stress equalization and consequently a greater failure load.

In both these specimens an early yielding of the tensile tube wall in the area along the weld to the vertical was indicated by a considerable peeling of the stress-coat. For the zero-eccentricity joint cracking and final peeling of the stress-coat occurred in a load range of 70 to 90 kips. For the joint with a negative eccentricity this load range was between 90 and 120 kips.

The total and elastic strains measured on the chord-member tube have been used to evaluate the principal stress directions. The results are presented in Figures 18, 19, and 20, and clearly indicate the stress flow from the chord member into the web members. The isotropic-stress points are extrapolated from the stress-coat results, which are shown in Figures 21, 22, and 23. The direction of the lines tracing the cracks in the coat were in complete agreement with those obtained from the strain-gage results, although the stress-coat and the gages were used on two different sides of the tube walls. The principal stress directions of the gages located close to the welds on the chord member showed small but consistent changes under increasing loads, indicating a redistribution of the load transferred through the welds.

The location of the isotropic points indicates a correlation between the narrowing of the compressive-stress flow and the consequent increase of stress concentration leading to an accelerated failure of the chord tube particularly and the joint in general.

VI. Summary and Conclusions

Three welded joints of a two-dimensional truss, built from steel tubes, were loaded to failure. Each joint was composed of a chord member and a vertical web member, both under compression, and a 45°-diagonal web member under tension. The members had the following dimensions:

Chord member	O. D. = 12 3/4 in.	wall thickness = 1/4 in.
Vertical web member	O. D. = 6 5/8 in.	wall thickness = 3/8 in.
Diagonal web member	O. D. = 6 5/8 in.	wall thickness = 3/16 in.

The effect of the eccentricity between the resultant web-member forces and the axial component of chord-member force was investigated by changing the geometric arrangements of the joints, (see Figures 2, 3, and 4), namely:

Positive eccentricity = + (1/4) (12 3/4) = + 3 3/16 in.

Zero eccentricity = 0 in.

Negative eccentricity = - (1/4) (12 3/4) = - 3 3/16 in.

As expected, an affect of eccentricity on ultimate failure load was found, i.e.:

Positive-eccentricity joint: $P_{failure}$ = 137 kips (50%)

Zero-Eccentricity joint: $P_{failure}$ = 209 kips (75%)

Negative-eccentricity joint: $P_{failure}$ = 277 kips (100%)

These results indicated that the failure load increased as a result of the larger intersection between the web-member wall surfaces and the subsequent welding area. As a result of the increased intersection the strain and stress results indicated a progressively more uniform load distribution in the web members next to the welds.

Comparing these failure loads with the failure load of an identical tube under tension shows the excellent capacity of the negative-eccentricity joint to transfer a load even greater than the single member. Since the failure in tension of a single tube--with O. D. = 6 5/8 in. and t = 3/16 in.--was 255 kips, the following strength factors for the joints were determined:

Positive-eccentricity joint: Joint strength factor = 0.54

Zero-eccentricity joint: Joint strength factor = 0.82

Negative-eccentricity joint: Joint strength factor = 1.08

These factors clearly show the favorable performance of the tested negative eccentricity joint.

It should be emphasized here that, although the results of the eccentricity affect investigated in this program undoubtedly represents a general tendency, the obtained percentages cannot be transferred to other member sizes and joint arrangements. If the chord-member wall had been thicker, the 137-kip failure load would probably have been greater. For web members with smaller outer diameters but identical areas, the joint strength for the zero- and negative-joint eccentricities would not have been so effective.

To evaluate these influences, further tests are necessary in which the affect of the chord-member wall thickness, the diameter-ratio of the chord and web members, and the eccentricity would be investigated.

VII. Organization

The work reported herein was conducted in the Structural Engineering Materials Laboratory, Division of Structural Engineering and Structural Mechanics, Department of Civil Engineering, University of California, Berkeley. The program was made possible by grants-in-aid from the Shell Development Company, Exploration and Production Research Division, at Houston, and the Standard Oil Company of California, Engineering Department, San Francisco.

The author wishes to thank his research assistant, Roy McBain Stephen, graduate student in Structural Engineering and Structural Mechanics, for his valuable assistance in the execution of this program.

TABLE I. TOTAL AND ELASTIC STRAINS IN MICROINCHES/IN. AND AXIAL AND TANGENTIAL STRESSES IN PSI FOR THE WEB-MEMBERS

Positive-Eccentricity Joint

COMPRESSION MEMBER (Gages Nos. 1, 2, 5, and 6)

Load	90^k		120^k	
	$\varepsilon_{tot.}$	$\varepsilon_{el.}$	$\varepsilon_{tot.}$	$\varepsilon_{el.}$
$\varepsilon_1=\varepsilon_{axial}$	+90	+85	+215	+90
$\varepsilon_2=\varepsilon_{tang}$	-50	-50	-55	-110
σ_{axial}	+2,200		+1,700	
σ_{tang}	-700		-2,600	

Load	90^k		120^k	
	$\varepsilon_{tot.}$	$\varepsilon_{el.}$	$\varepsilon_{tot.}$	$\varepsilon_{el.}$
$\varepsilon_5=\varepsilon_{axial}$	-460	-655	-580	-820
$\varepsilon_6=\varepsilon_{tang}$	-75	-150	-35	-165
σ_{axial}	-26,300		-28,600	
σ_{tang}	-12,000		-14,300	

TENSION MEMBER (Gages 13, 12, 17, and 18)

Load	90^k		120^k	
	$\varepsilon_{tot.}$	$\varepsilon_{el.}$	$\varepsilon_{tot.}$	$\varepsilon_{el.}$
$\varepsilon_{13}=\varepsilon_{axial}$	+1165	+1505	+2345	+2150
$\varepsilon_{12}=\varepsilon_{tang}$	+180	+240	+330	+245
σ_{axial}	+51,700		+75,000	
σ_{tang}	+24,200		+31,400	

Load	90^k		120^k	
	$\varepsilon_{tot.}$	$\varepsilon_{el.}$	$\varepsilon_{tot.}$	$\varepsilon_{el.}$
$\varepsilon_{17}=\varepsilon_{axial}$	+440	+470	+730	+705
$\varepsilon_{18}=\varepsilon_{tang}$	+35	+40	+95	+95
σ_{axial}	+15,800		+24,000	
σ_{tang}	+6,400		+10,800	

TABLE II. TOTAL AND ELASTIC STRAINS IN MICROINCHES/IN. AND AXIAL AND TANGENTIAL STRESSES IN PSI FOR THE WEB-MEMBERS

Zero-Eccentricity Joint

COMPRESSION MEMBER (Gages Nos. 1, 2, 13, and 12)

Load	70^k		130^k		160^k	
	$\varepsilon_{tot.}$	$\varepsilon_{el.}$	$\varepsilon_{tot.}$	$\varepsilon_{el.}$	$\varepsilon_{tot.}$	$\varepsilon_{el.}$
$\varepsilon_1 = \varepsilon_{axial}$	+45	+35	+140	+70	+215	+105
$\varepsilon_2 = \varepsilon_{tang}$	-20	-40	-20	-65	-55	-95
σ_{axial}	+700		+1,700		+2,400	
σ_{tang}	-1,000		-1,500		-2,000	
$\varepsilon_{13} = \varepsilon_{axial}$	-345	-445	-855	-845	-1370	-1090
$\varepsilon_{12} = \varepsilon_{tang}$	+260	+160	+630	+260	+850	+300
σ_{axial}	-12,800		-24,800		-32,300	
σ_{tang}	+400		-700		-2,100	

TENSION MEMBER (Gages Nos. 14, 15, 26, and 25)

$\varepsilon_{14} = \varepsilon_{axial}$	+2130	+975	+6760	+1410	+11035	+1380
$\varepsilon_{15} = \varepsilon_{tang}$	-390	-190	-4170	-570	-8640	-775
σ_{axial}	+29,900		+39,900		+36,600	
σ_{tang}	+4,400		-3,300		-10,300	
$\varepsilon_{26} = \varepsilon_{axial}$	+305	+275	+605	+570	+815	+755
$\varepsilon_{25} = \varepsilon_{tang}$	-55	-95	-130	-195	-125	-245
σ_{axial}	+8,000		+16,500		+22,000	
σ_{tang}	+2,000		-150		+250	

TABLE III. TOTAL AND ELASTIC STRAINS IN MICROINCHES/IN. AND AXIAL AND TANGENTIAL STRESSES IN PSI FOR THE WEB-MEMBERS

Negative-Eccentricity Joint

COMPRESSION MEMBER (Gages Nos. 1, 2, 13, and 12)

Load	70^k		150^k		180^k		210^k	
	$\varepsilon_{tot.}$	$\varepsilon_{el.}$	$\varepsilon_{tot.}$	$\varepsilon_{el.}$	$\varepsilon_{tot.}$	$\varepsilon_{el.}$	$\varepsilon_{tot.}$	$\varepsilon_{el.}$
$\varepsilon_1 = \varepsilon_{axial}$	+20	+25	+90	+30	+125	+35	+155	+40
$\varepsilon_2 = \varepsilon_{tang}$	-40	-40	+30	-50	+90	-55	+200	-60
σ_{axial}	+350		+450		+550		+700	
σ_{tang}	-1,000		-1,300		-1,400		-1,500	
$\varepsilon_{13} = \varepsilon_{axial}$	-175	-215	-440	-440	-585	-525	-780	-650
$\varepsilon_{12} = \varepsilon_{tang}$	+155	+150	+415	+360	+590	+435	+840	+510
σ_{axial}	-5,400		-10,500		-12,400		-15,700	
σ_{tang}	+2,600		+7,000		+8,500		+9,600	

COMPRESSION MEMBER (Gauge Nos. 1, 2, 13, and 12)

$\varepsilon_{14} = \varepsilon_{axial}$	+515	+470	+2435	+1100	+5400	+1410	+14770	+1760
$\varepsilon_{15} = \varepsilon_{tang}$	-175	-200	-1045	-460	-2200	-600	-6460	-750
σ_{axial}	+8,800		+30,900		+39,500		+49,300	
σ_{tang}	-1,600		-3,100		-4,300		-5,300	
$\varepsilon_{26} = \varepsilon_{axial}$	+470	+385	+1030	+770	+1245	+920	+2005	+990
$\varepsilon_{25} = \varepsilon_{tang}$	-10	-40	-15	-95	+30	-120	+60	-160
σ_{axial}	+12,100		+24,100		+28,700		+30,600	
σ_{tang}	+2,900		+5,300		+6,100		+5,600	

TABLE IV. PRINCIPAL STRESSES IN PSI FOR THE WEB-MEMBERS UNDER DIFFERENT LOADS

Positive-Eccentricity Joint

COMPRESSION MEMBER

$P = 90^k$

	Gages 1-2	Gages 7-8-9	Gages 5-6
σ_1	+2,200*	-8,200	-12,000
σ_2	-700	-11,300	-26,300*

$P = 120^k$

	Gages 1-2	Gages 7-8-9	Gages 5-6
σ_1	+1,700*	-14,400	-14,300
σ_2	-2,600	-23,100	-28,600*

TENSION MEMBER

$P = 90^k$

	Gages 12-13	Gages 14-15-16	Gages 17-18
σ_1	+51,700	+37,000	+15,800
σ_2	+24,200	+16,000	+6,400

$P = 120^k$

	Gages 12-13	Gages 14-15-16	Gages 17-18
σ_1	+75,000	+53,500	+24,000
σ_2	+31,400	+21,600	+10,800

* axial stress

TABLE V. PRINCIPAL STRESSES IN PSI FOR THE WEB MEMBER UNDER DIFFERENT LOADS

Zero-Eccentricity Joint

COMPRESSION MEMBER

	Gages 1-2	Gages 3-4-5	Gages 6-7-8	Gages 9-10-11	Gages 12-13
$P = 70^k$					
σ_1	+700*	-3,400	-6,700	-7,800	+400
σ_2	-1,000	-4,700	-9,000	-16,300	-12,800*
$P = 130^k$					
σ_1	+1,700*	-5,100	-15,700	-16,000	-700
σ_2	-1,500	-7,700	-16,600	-27,500	-24,800*
$P = 160^k$					
σ_1	+2,400*	-5,900	-14,300	-20,900	-2,100
σ_2	-2,000	-9,900	-21,000	-35,200	-32,300*

* axial stress

TENSION MEMBER

	Gages 14-15	Gages 16-17-18	Gages 19-20-21	Gages 22-23-24	Gages 25-26
$P = 70^k$					
σ_1	+29,900	+31,400	+16,000	+17,000	+8,000
σ_2	+4,400	-5,500	+4,500	+6,800	+2,000
$P = 130^k$					
σ_1	+39,900	+55,400	+32,300	+35,800	+16,500
σ_2	-3,300	-16,800	+6,200	+12,800	-150
$P = 160^k$					
σ_1	+36,000	+74,000	+38,600	+46,500	+22,000
σ_2	-10,300	-32,000	+7,900	+16,000	+250

TABLE VI. PRINCIPAL STRESSES IN PSI FOR THE WEB MEMBERS UNDER DIFFERENT LOADS

Negative-Eccentricity Joint

COMPRESSION MEMBER

	Gages 1-2	Gages 3-4-5	Gages 6-7-8	Gages 9-10-11	Gages 12-13
$P = 70^k$					
σ_1	+350*	-5,800	-2,200	-5,400	+2,600
σ_2	-1,000	-11,300	-8,400	-11,100	-5,400*
$P = 150^k$					
σ_1	+450	-9,600	-4,100	-12,300	+7,000
σ_2	-1,300	-22,300	-19,600	-26,200	-10,500*
$P = 180^k$					
σ_1	+500*	-10.700	-4,400	-14,000	+8,500
σ_2	-1,400	-26,500	-24,200	-32,800	-12,400*
$P = 210^k$					
σ_1	+700*	-11,600	-4,100	-17,700	+9,600
σ_2	-1,500	-30,800	-28,800	-38,400	-15,700*

TENSION MEMBER

	Gages 14-15	Gages 16-17-18	Gages 19-20-21	Gages 22-23-24	Gages 25-26
$P = 70^k$					
σ_1	+8,800	+17,700	+18,800	+28,000	+12,100
σ_2	-1,600	+4,200	-6,400	+8,800	+2,900
$P = 150^k$					
σ_1	+30,900	+43,100	+44,500	+59,300	+24,100
σ_2	-3,100	+10,100	-16,500	+16,100	+5,300
$P = 180^k$					
σ_1	+39,500	+54,000	+58,500	+71,000	+28,700
σ_2	-4,300	+13,200	-22,400	+17,700	+6,100
$P = 210^k$					
σ_1	+49,300	+70,800	+78,000	+80,500	+30,600
σ_2	-5,300	+22,000	-30,800	+17,300	+5,600

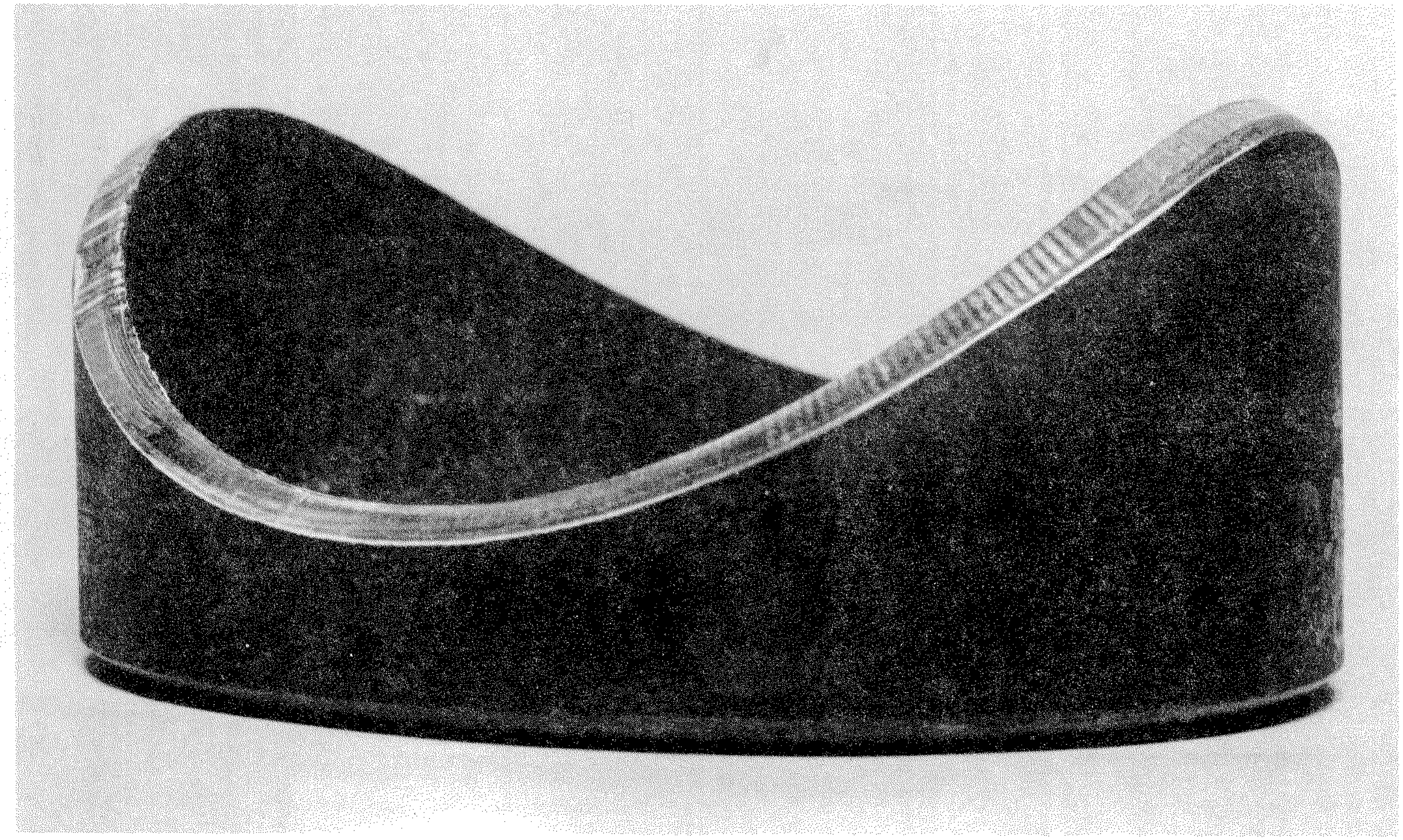

AUTOMATICALLY CUT TUBE

FIG. 1

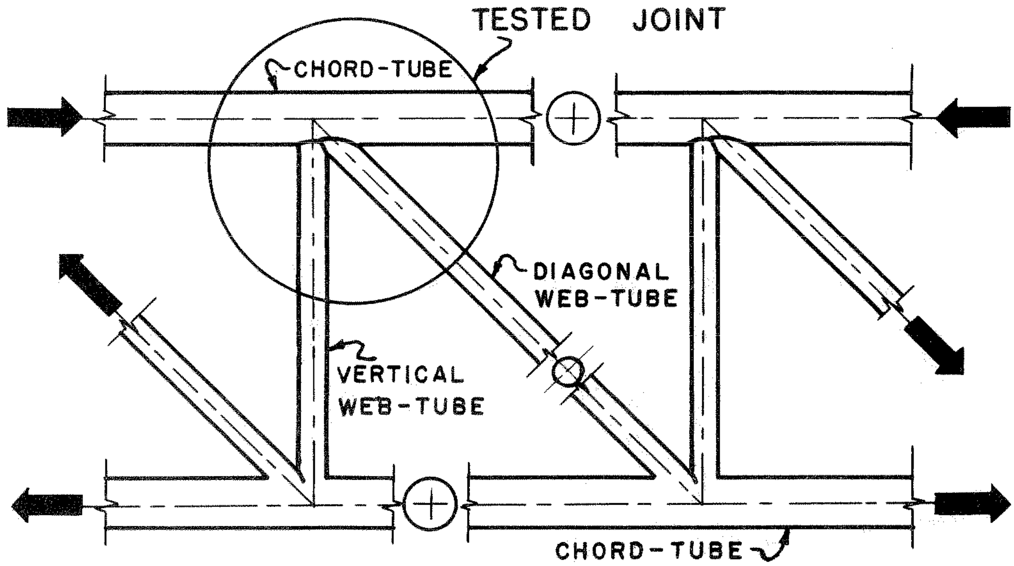

TUBE TRUSS WITH BASIC MEMBER FORCES
(ZERO ECCENTRICITY)

FIG. 2

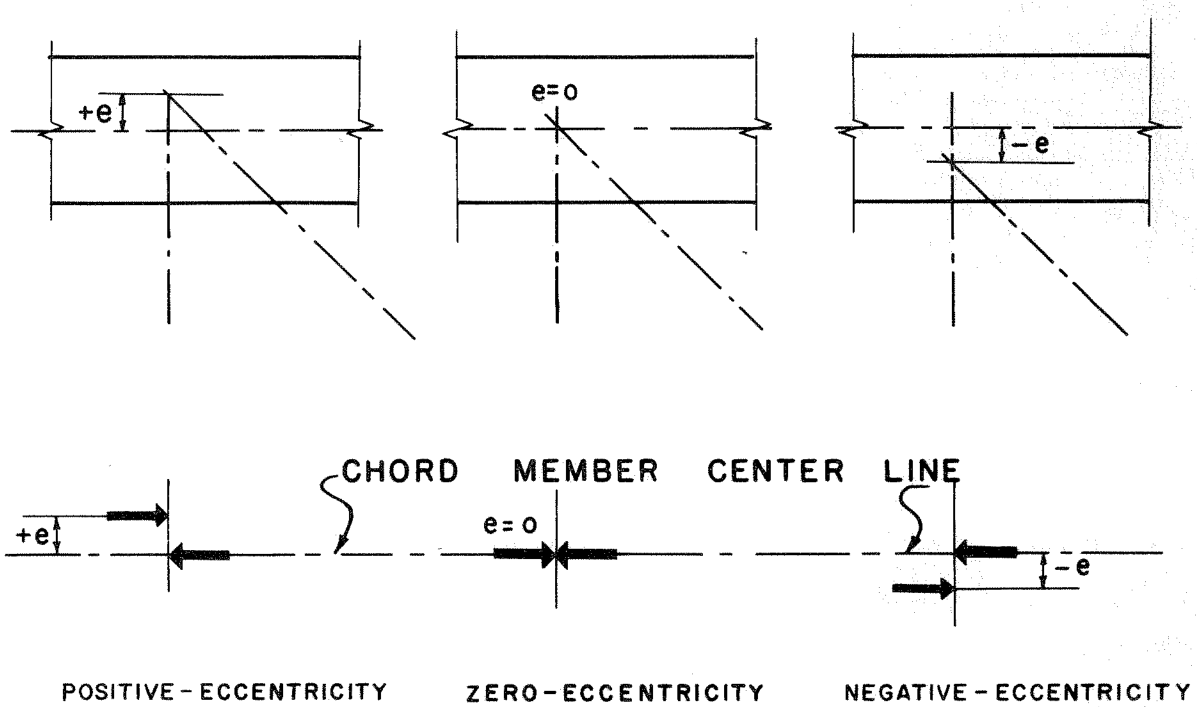

DIFFERENT JOINT ECCENTRICITIES AND RESULTING FORCE-EFFECTS

FIG. 3

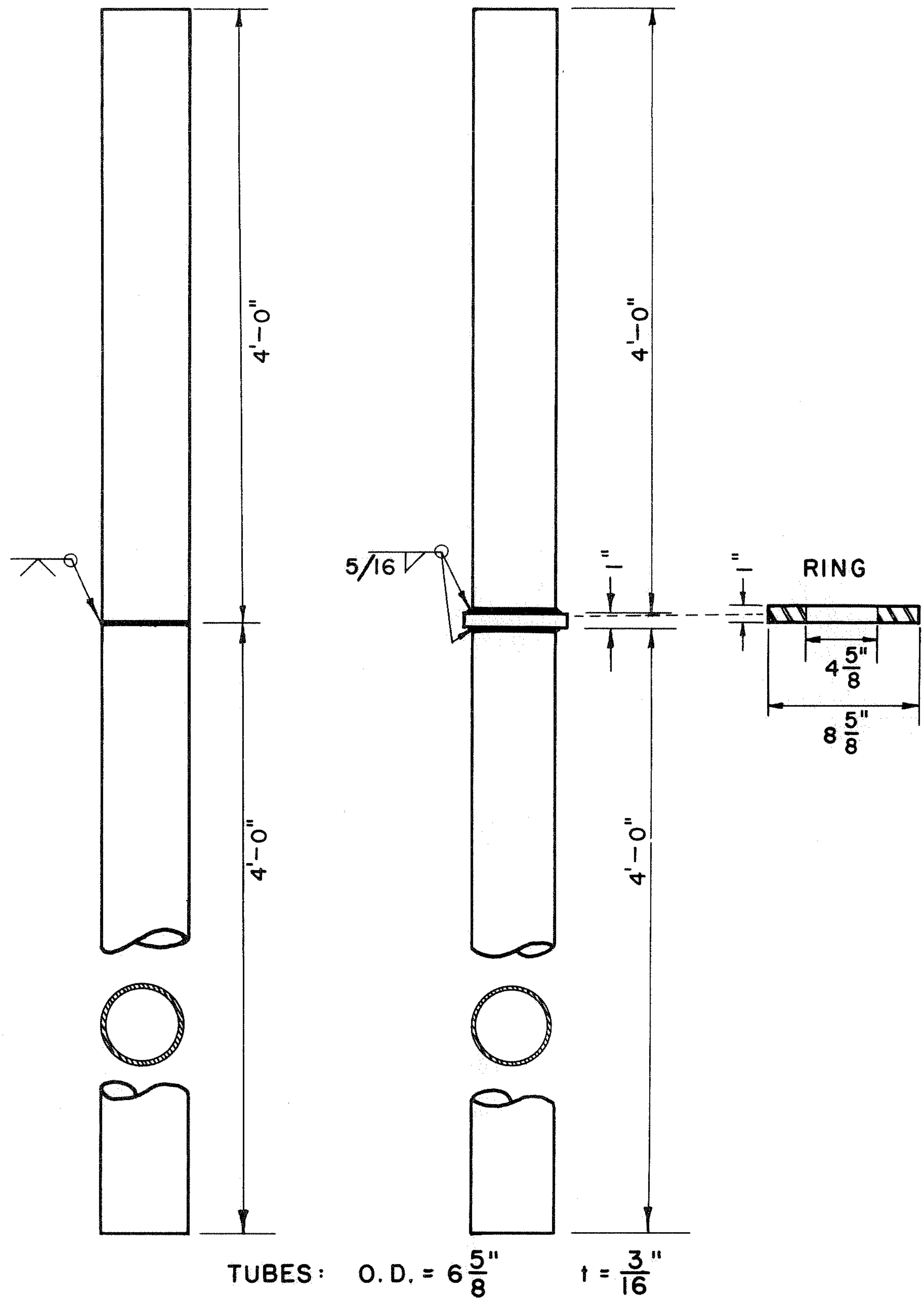

FIG. 4 — TENSILE TUBULAR TEST SPECIMENS

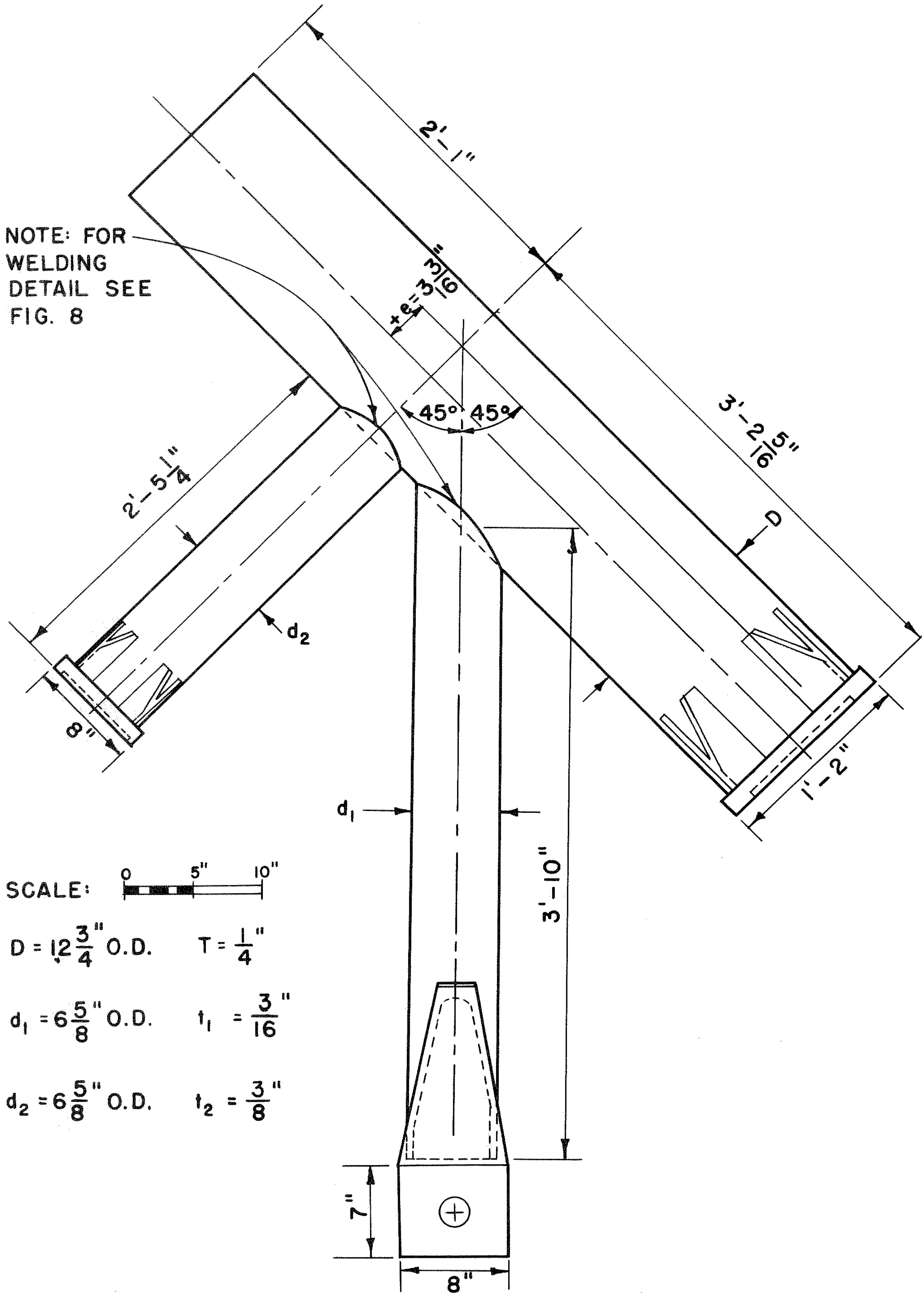

FIG. 5 — POSITIVE - ECCENTRICITY JOINT

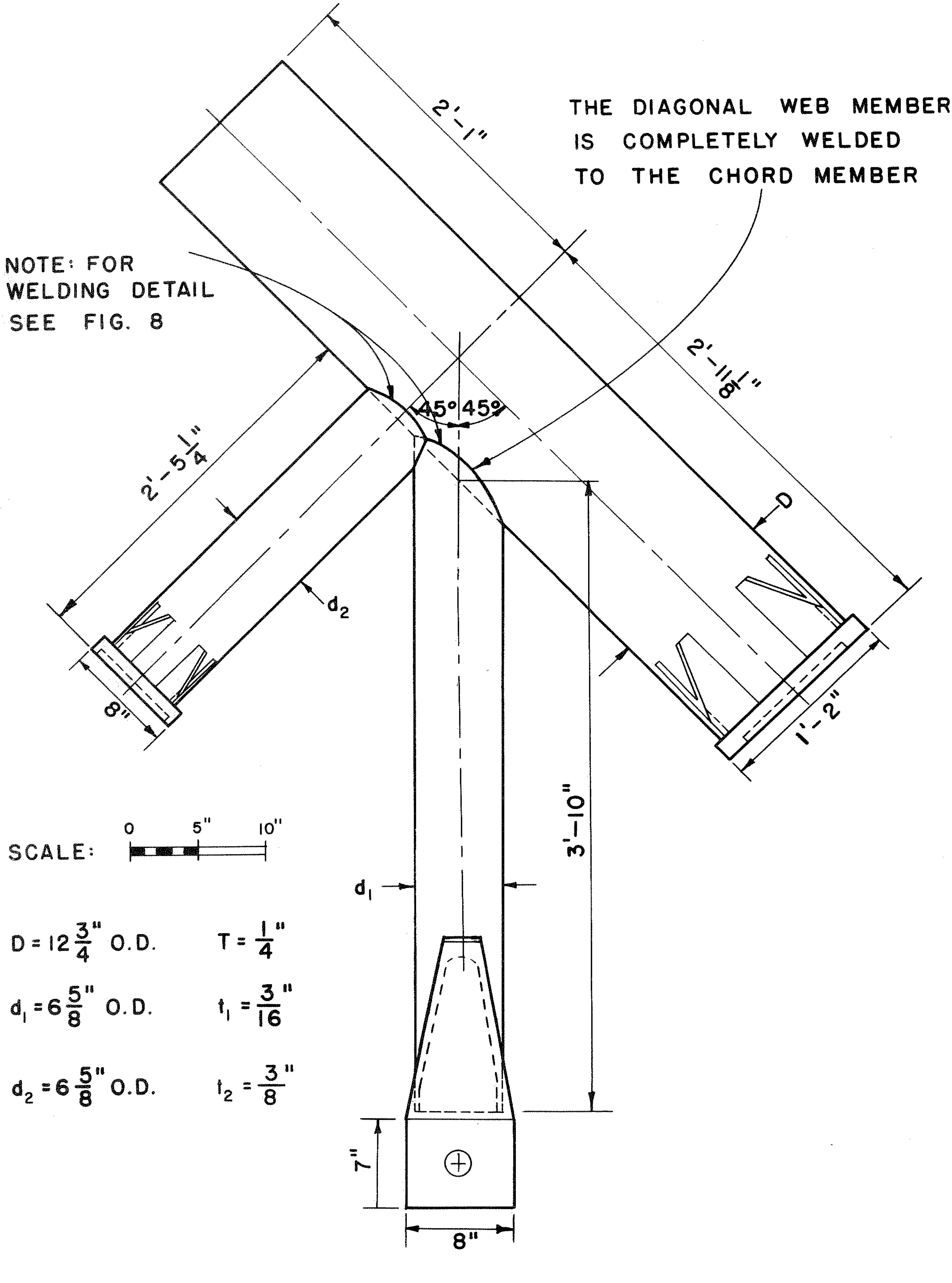

FIG. 6 — ZERO - ECCENTRICITY JOINT

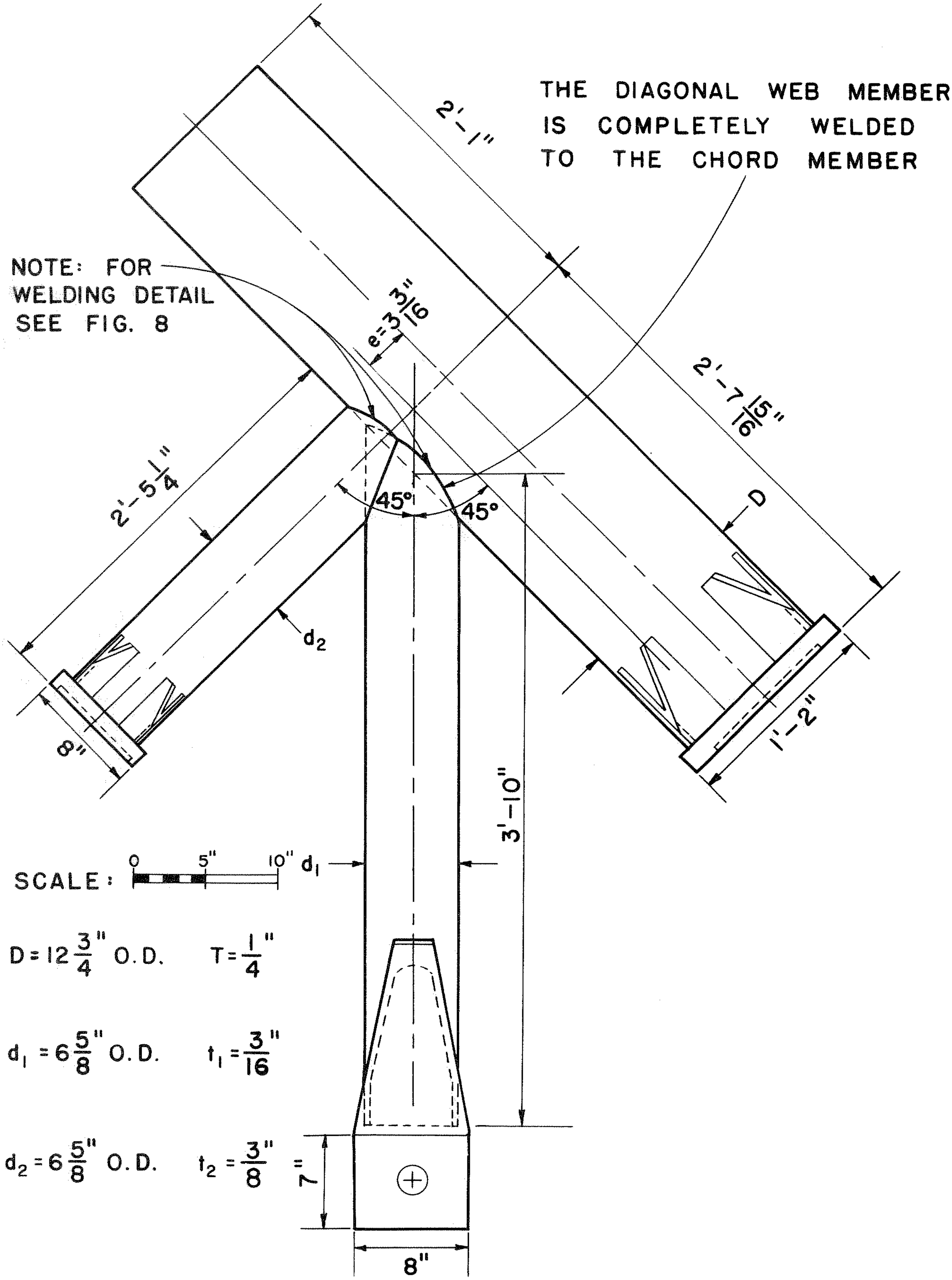

FIG. 7 - NEGATIVE - ECCENTRICITY JOINT

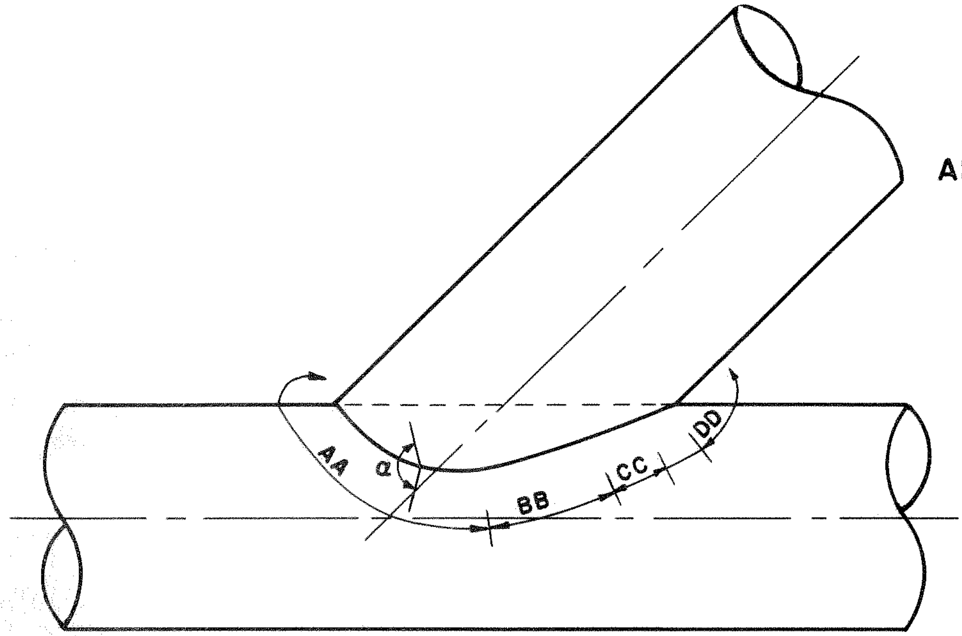

TYPICAL CONNECTION ELEVATION

ANGLE α IS MEASURED PERPENDICULAR TO JOINT LINE AND ON THE OUTSIDE OF PIPE

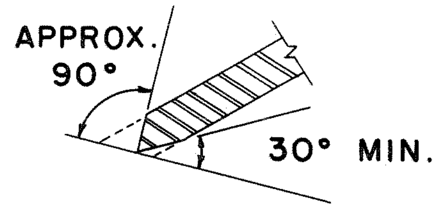

TRANSITION FROM DETAIL CC TO DD BY GRADUAL UNIFORM BEVELING

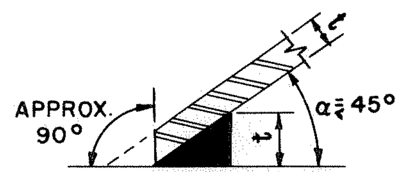

MAKE PENETRATION AS COMPLETE AS POSSIBLE

DD

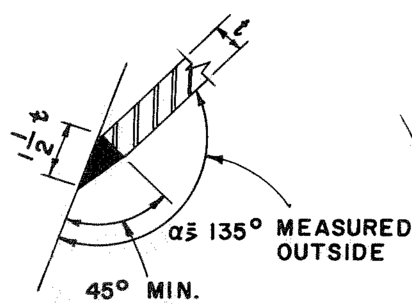

AA

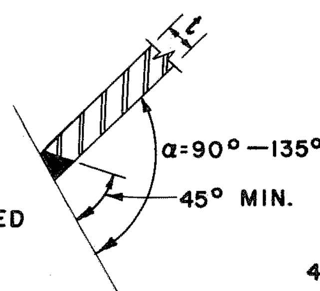

BB

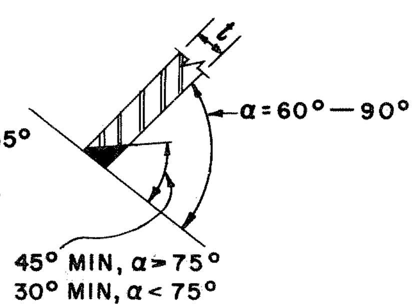

CC

DETAILS OF WELD FROM ONE SIDE ONLY

FIG. 8 — WELDING DETAILS

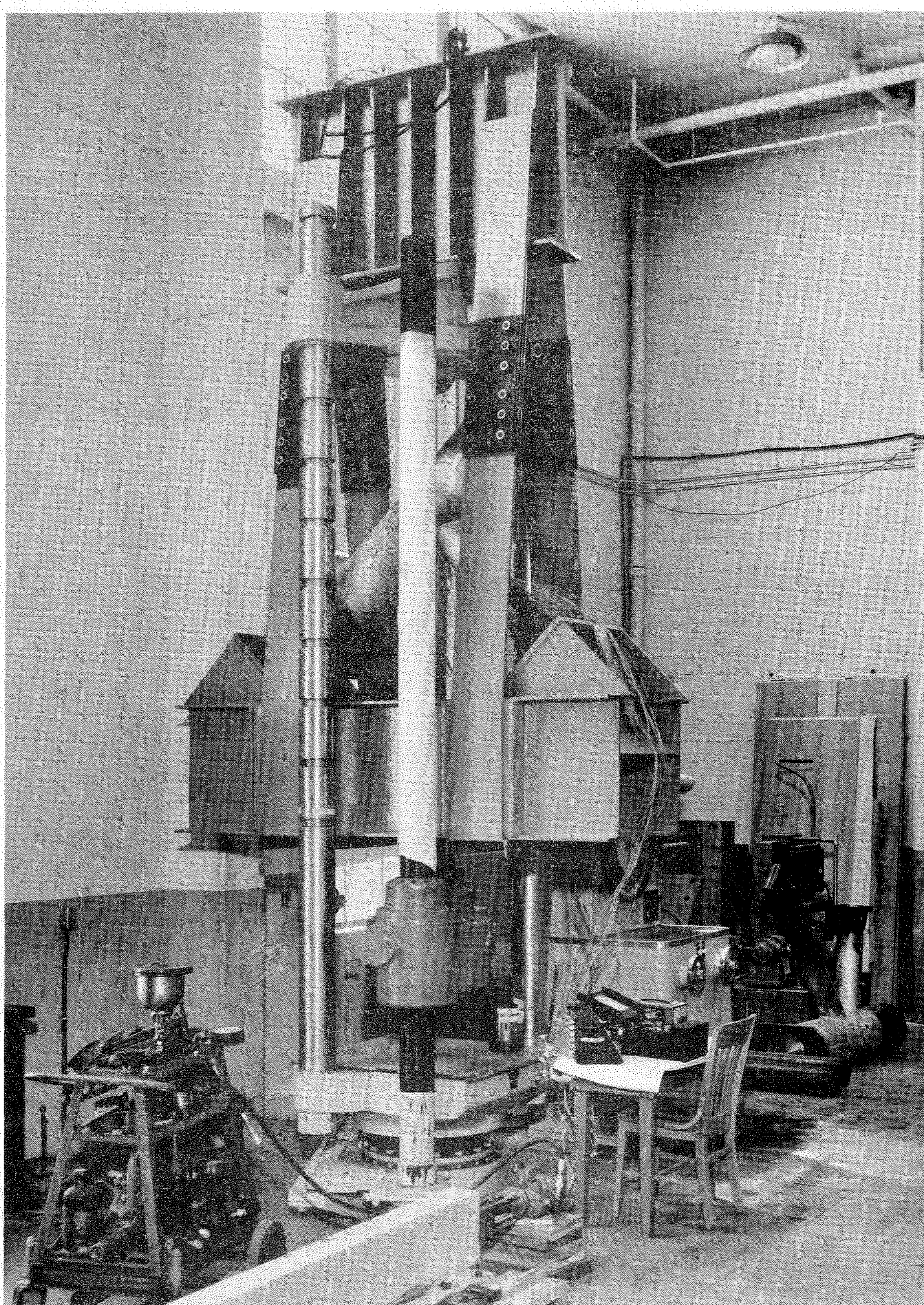

LOADING FRAME WITH JOINT-SPECIMEN MOUNTED IN 400,000-LB TESTING MACHINE

FIG. 9

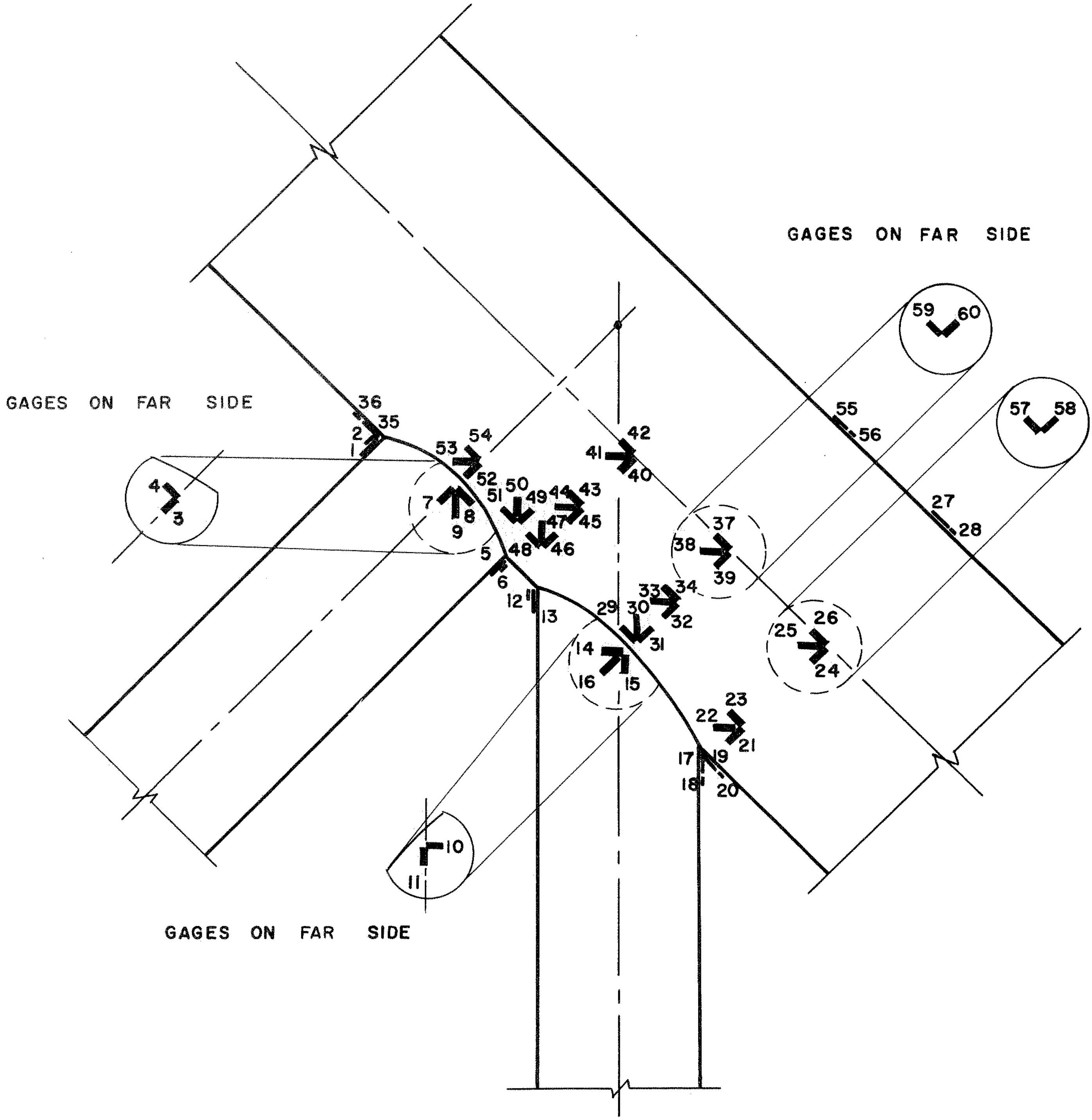

ARRANGEMENT OF STRAIN - GAGES

(POSITIVE-ECCENTRICITY JOINT)

FIG. 10

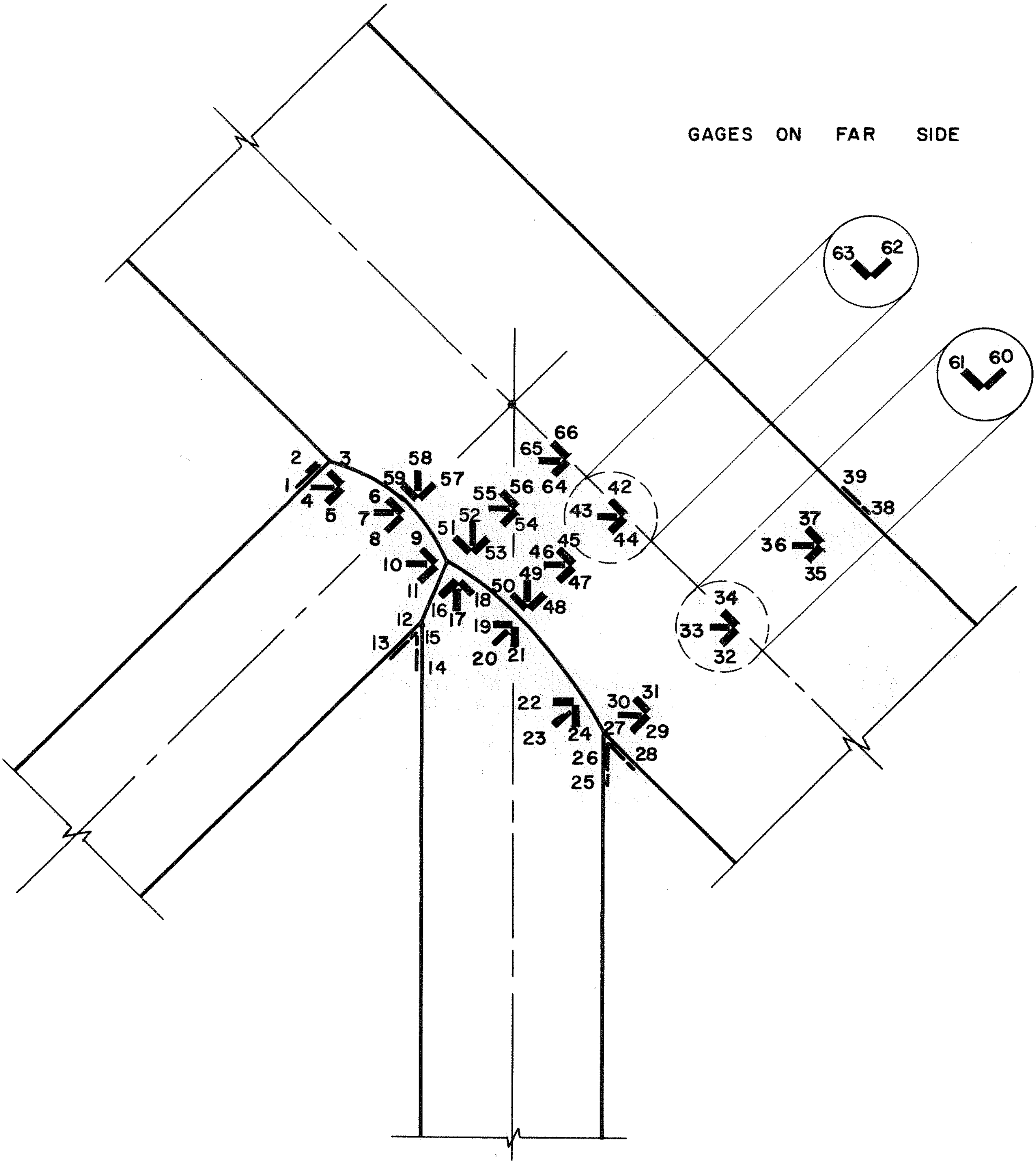

ARRANGEMENT OF STRAIN-GAGES
(ZERO-ECCENTRICITY JOINT)

FIG. 11

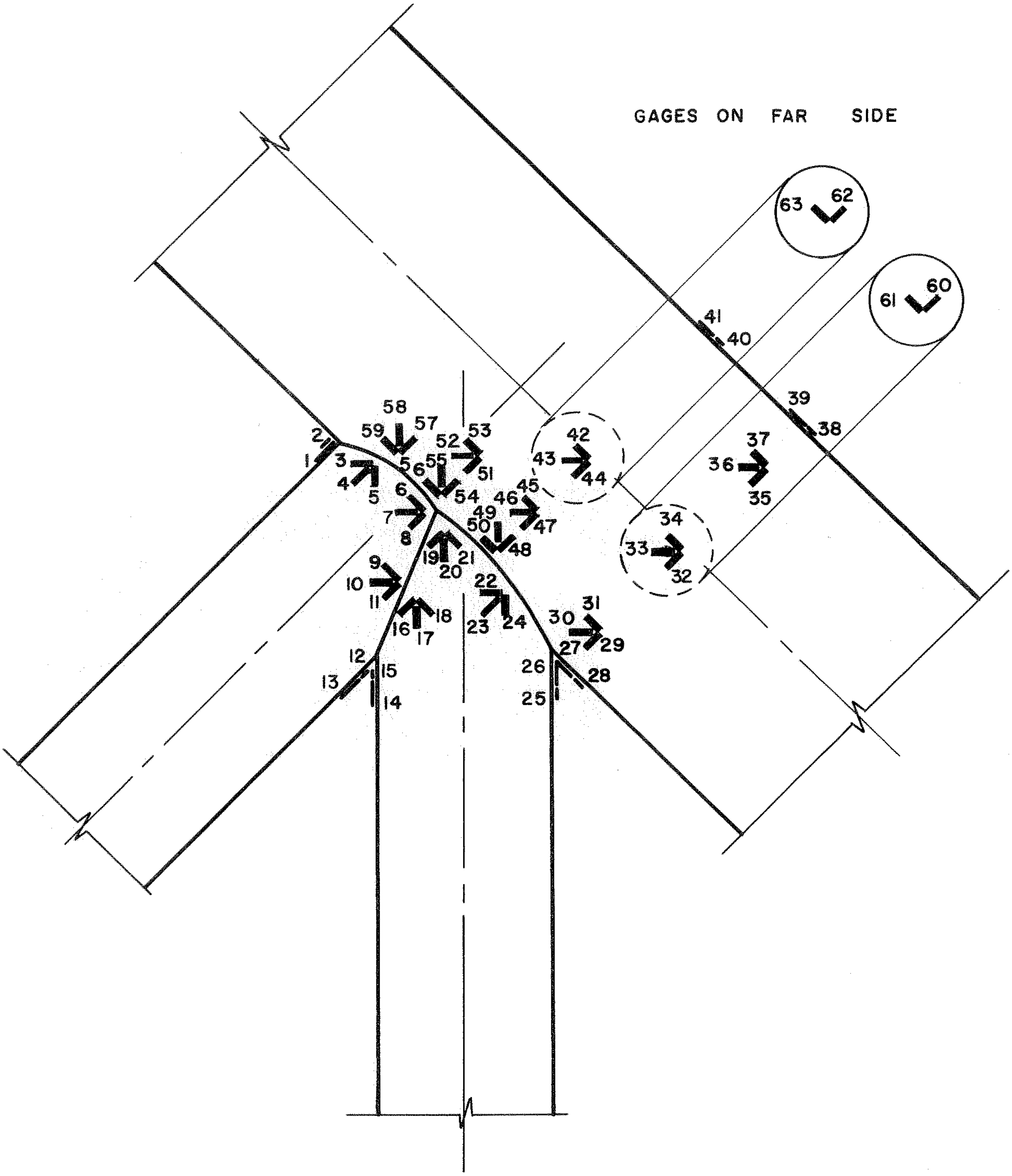

ARRANGEMENT OF STRAIN-GAGES

(NEGATIVE - ECCENTRICITY JOINT)

FIG. 12

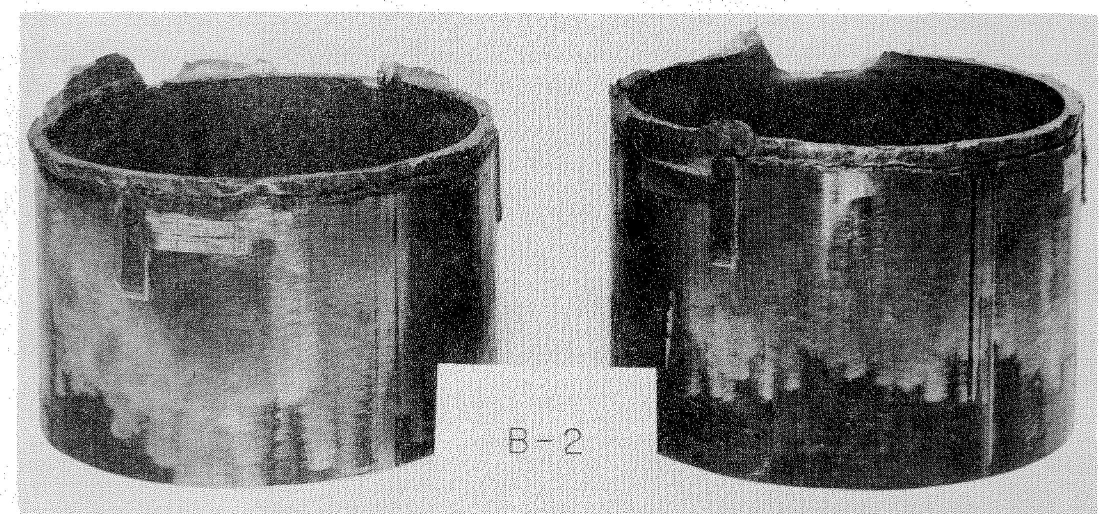

13 a

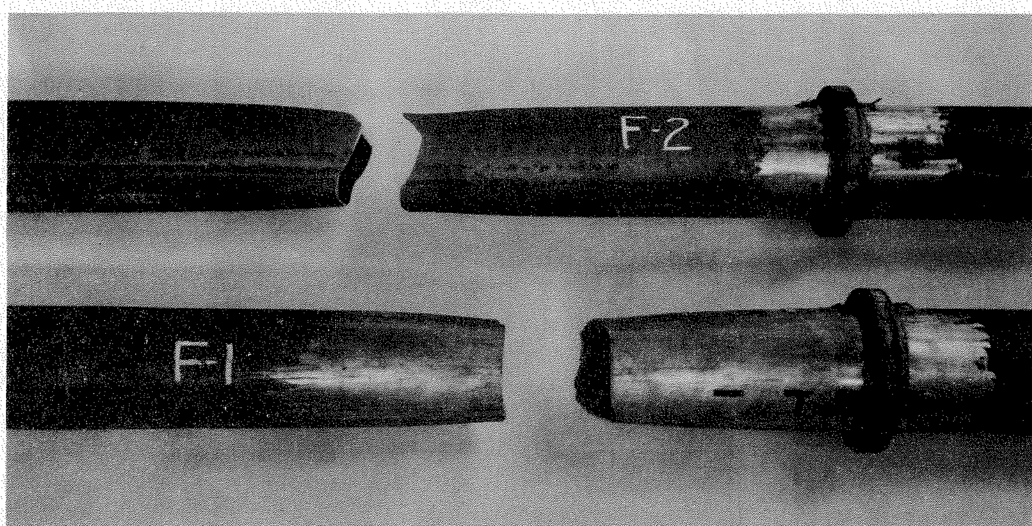

13 b

FRACTURED TEST TUBES (O.D.= 6 5/8 IN.)

FIG. 13

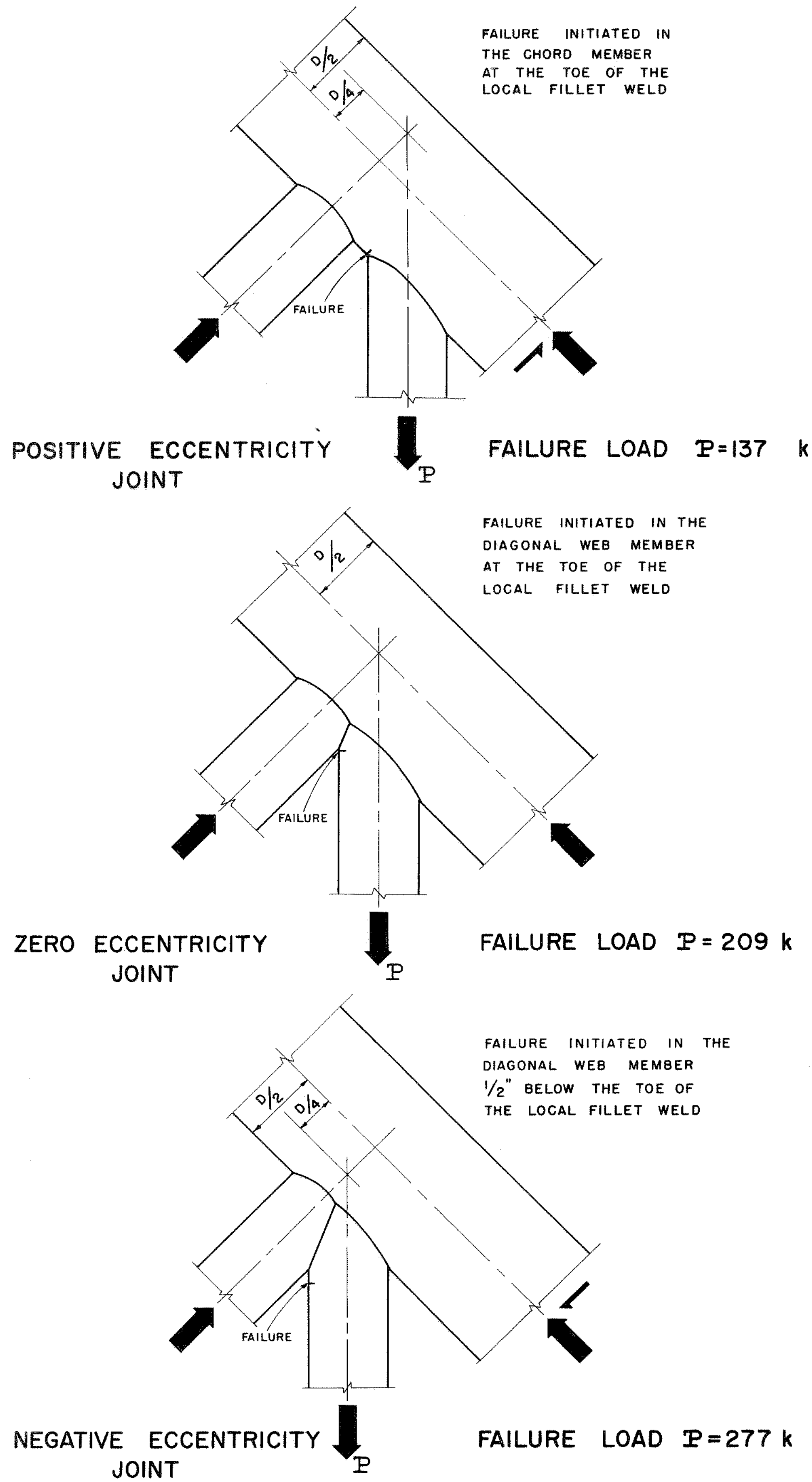

LOCATION OF INITIAL FAILURE OF JOINTS

FIG. 14

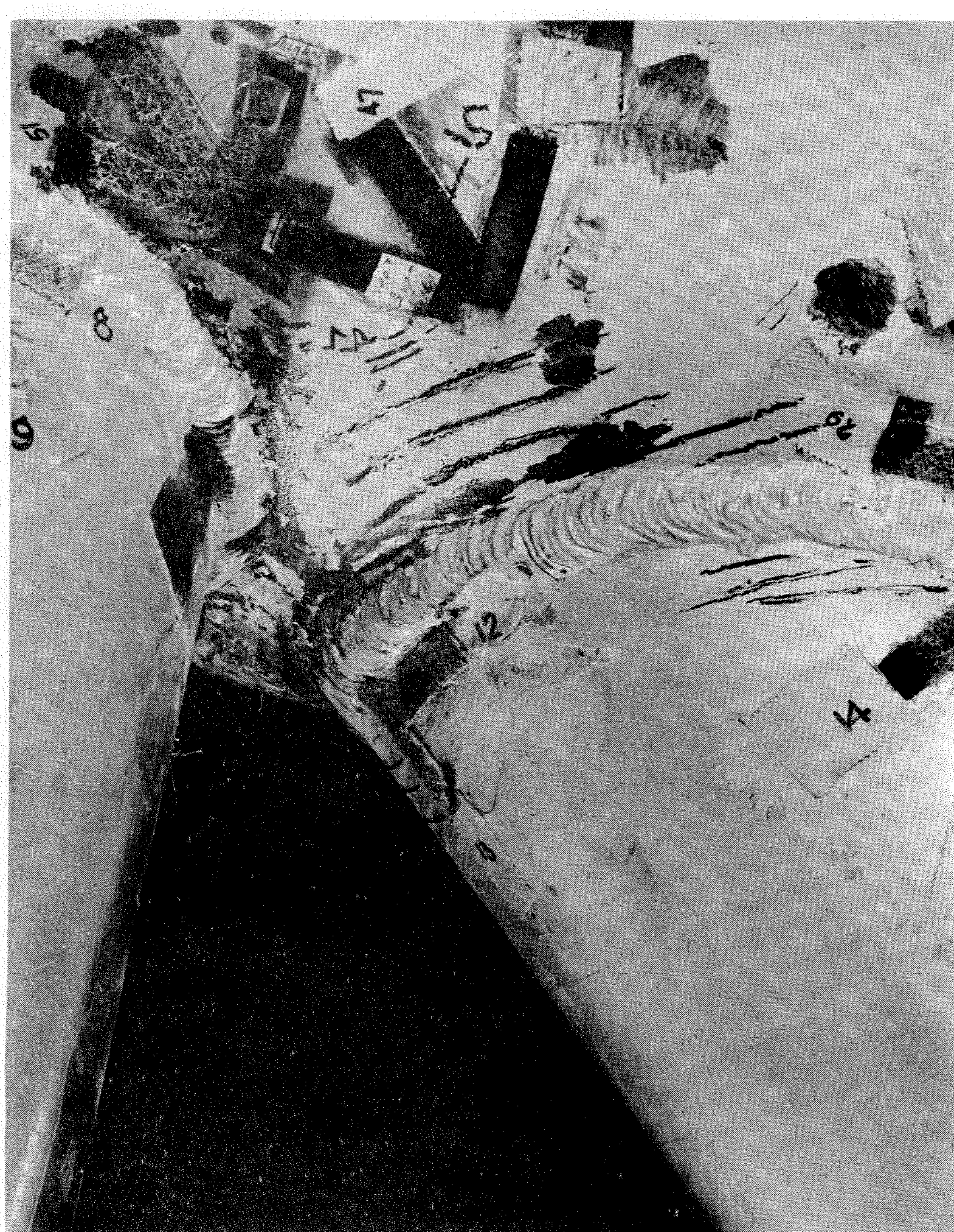

LOCAL FRACTURE IN CHORD-TUBE WALL AT TOE OF WELD

FIG. 15

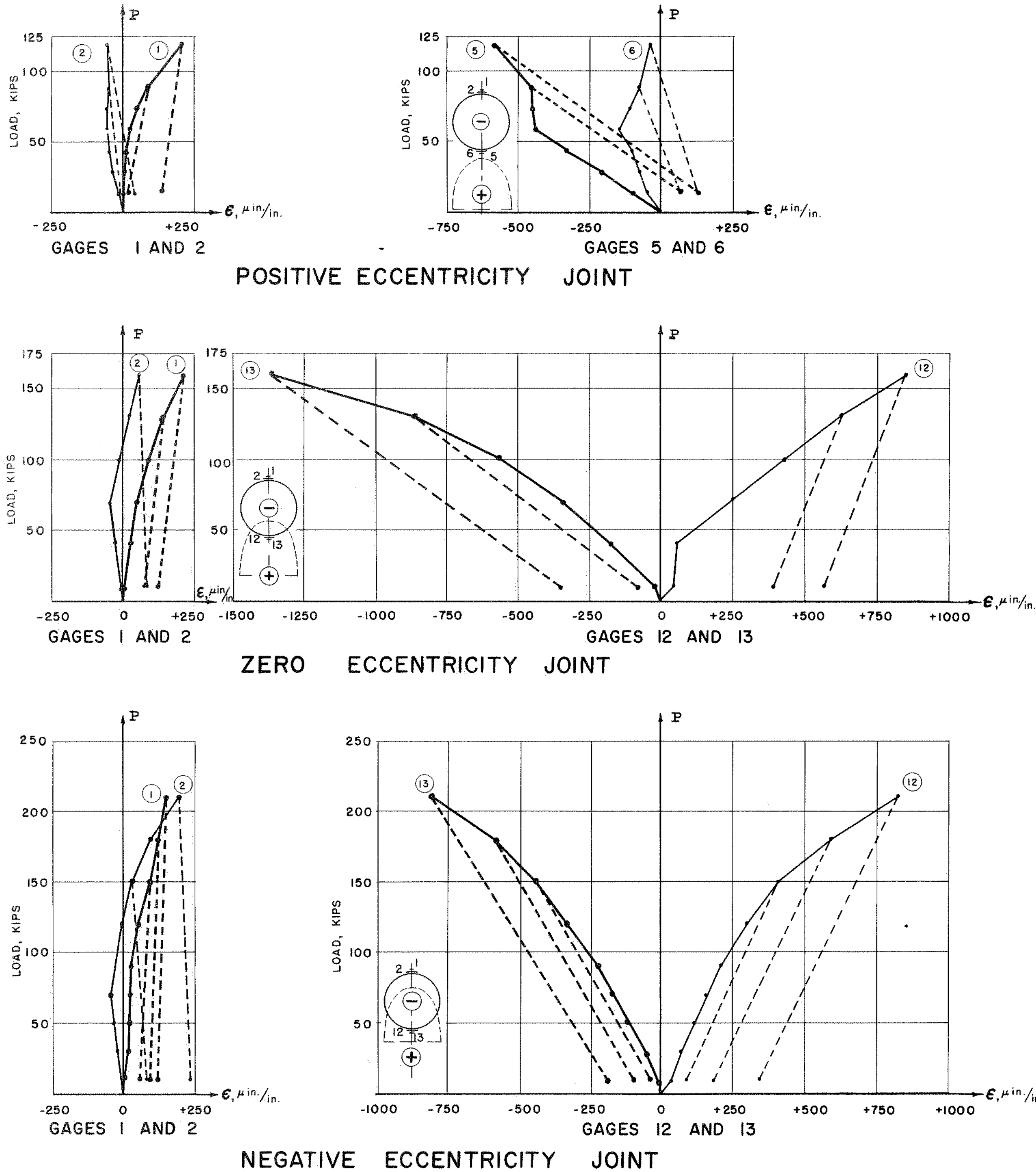

STRAINS IN MICRO-INCHES / INCH FOR GAGES ON COMPRESSION WEB MEMBER

FIG. 16

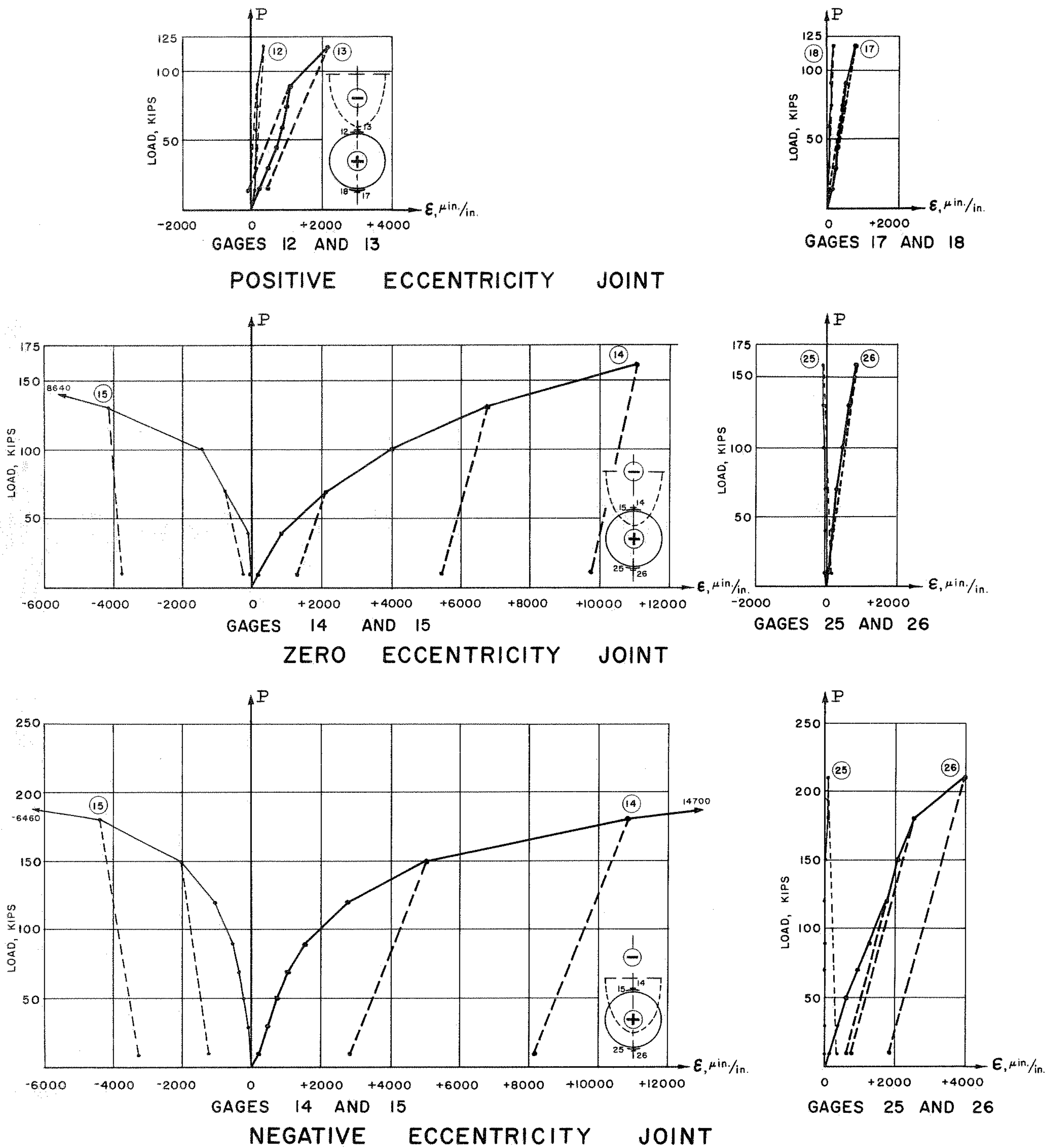

STRAINS IN MICRO-INCHES / INCH FOR

GAGES ON TENSION WEB MEMBER

FIG. 17

THE INDICATED ANGLES ARE STRESS-DIRECTIONS ON THE TUBE WALL, AND ARE MEASURED WITH RESPECT TO THE LOCAL AXIAL LINE.

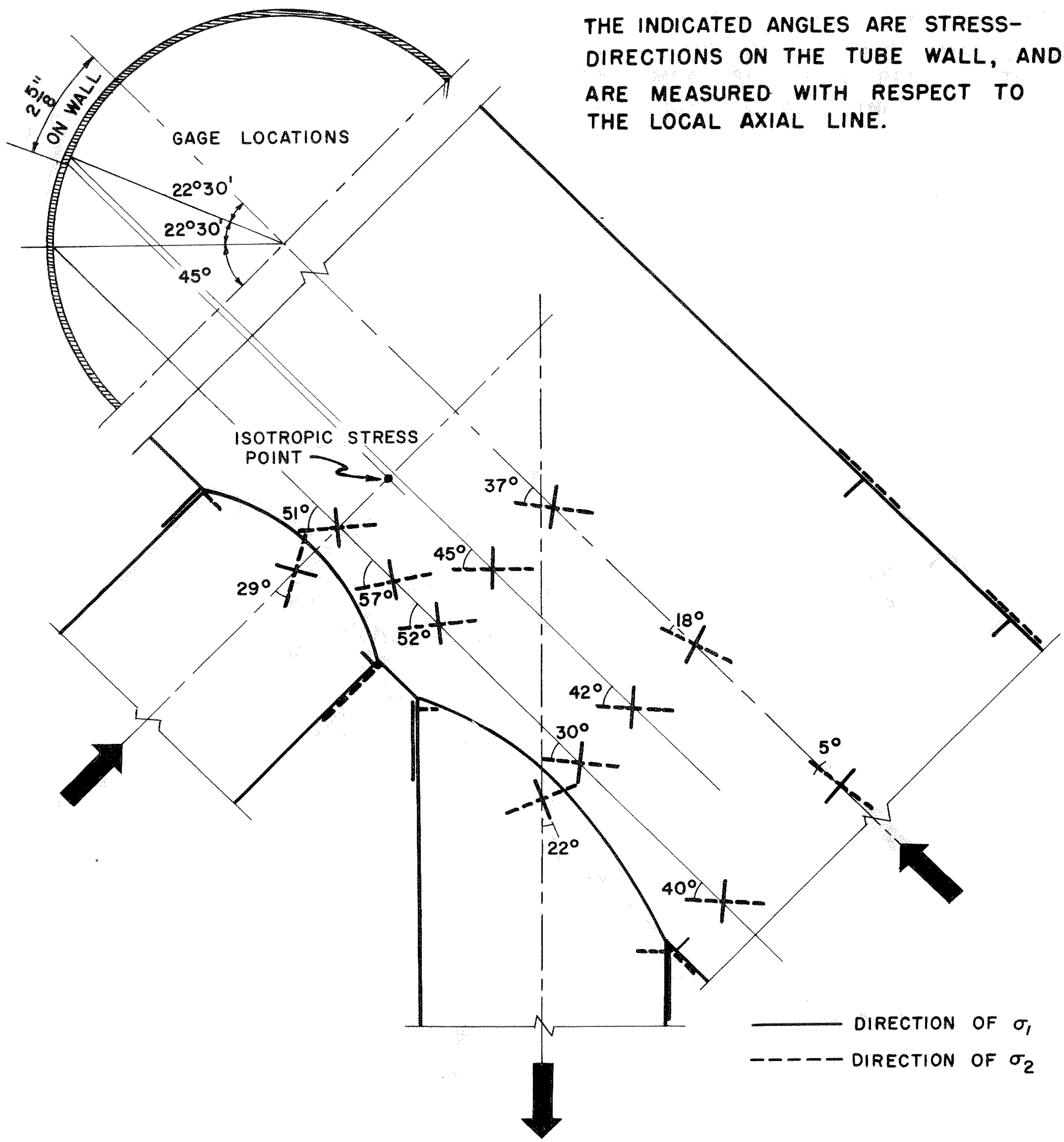

PRINCIPAL STRESS-DIRECTIONS AT GAGE LOCATIONS

(POSITIVE - ECCENTRICITY JOINT)

FIG. 18

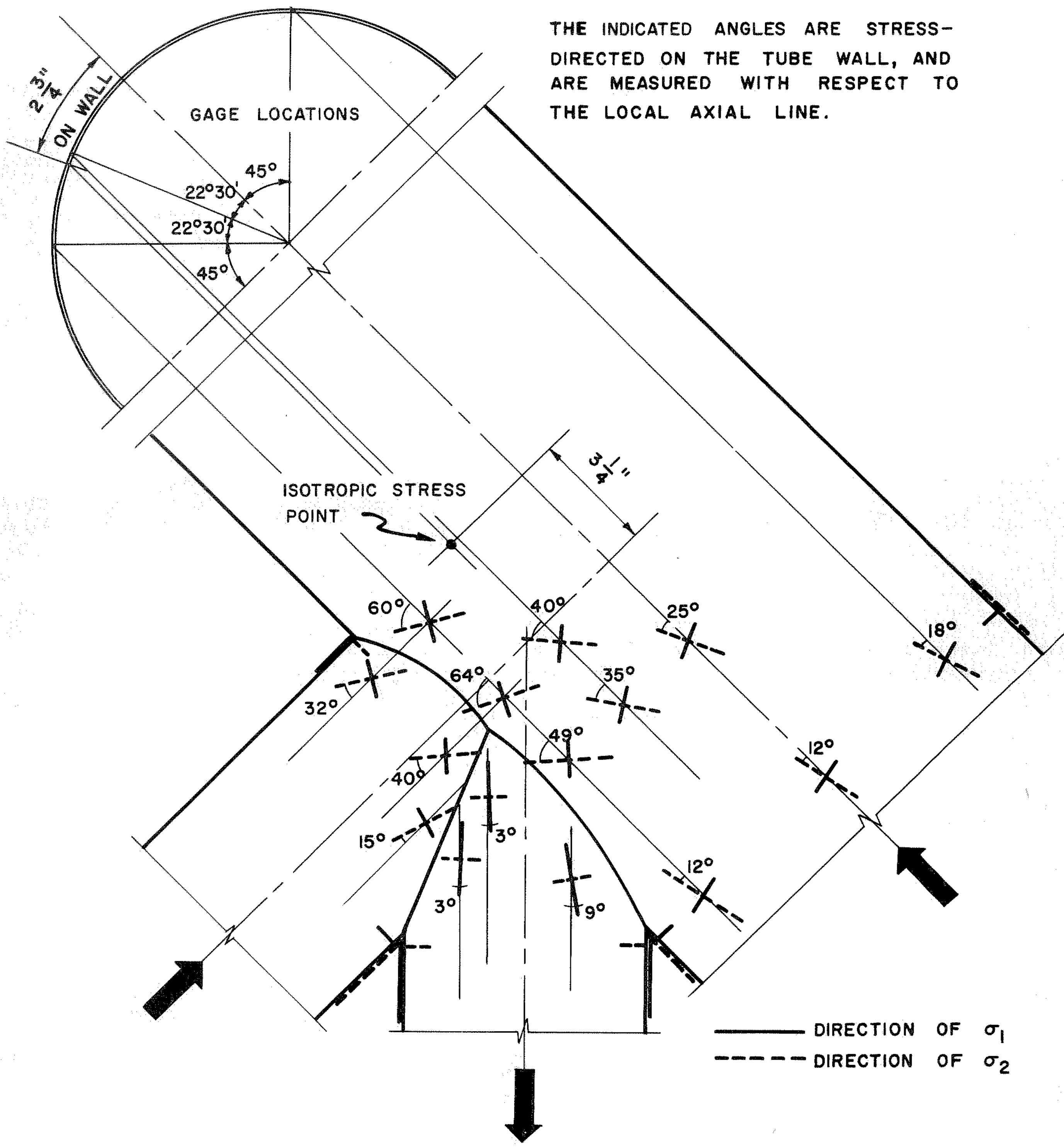

PRINCIPAL STRESS-DIRECTIONS AT GAGE LOCATIONS

(NEGATIVE ECCENTRICITY JOINT)

FIG. 20

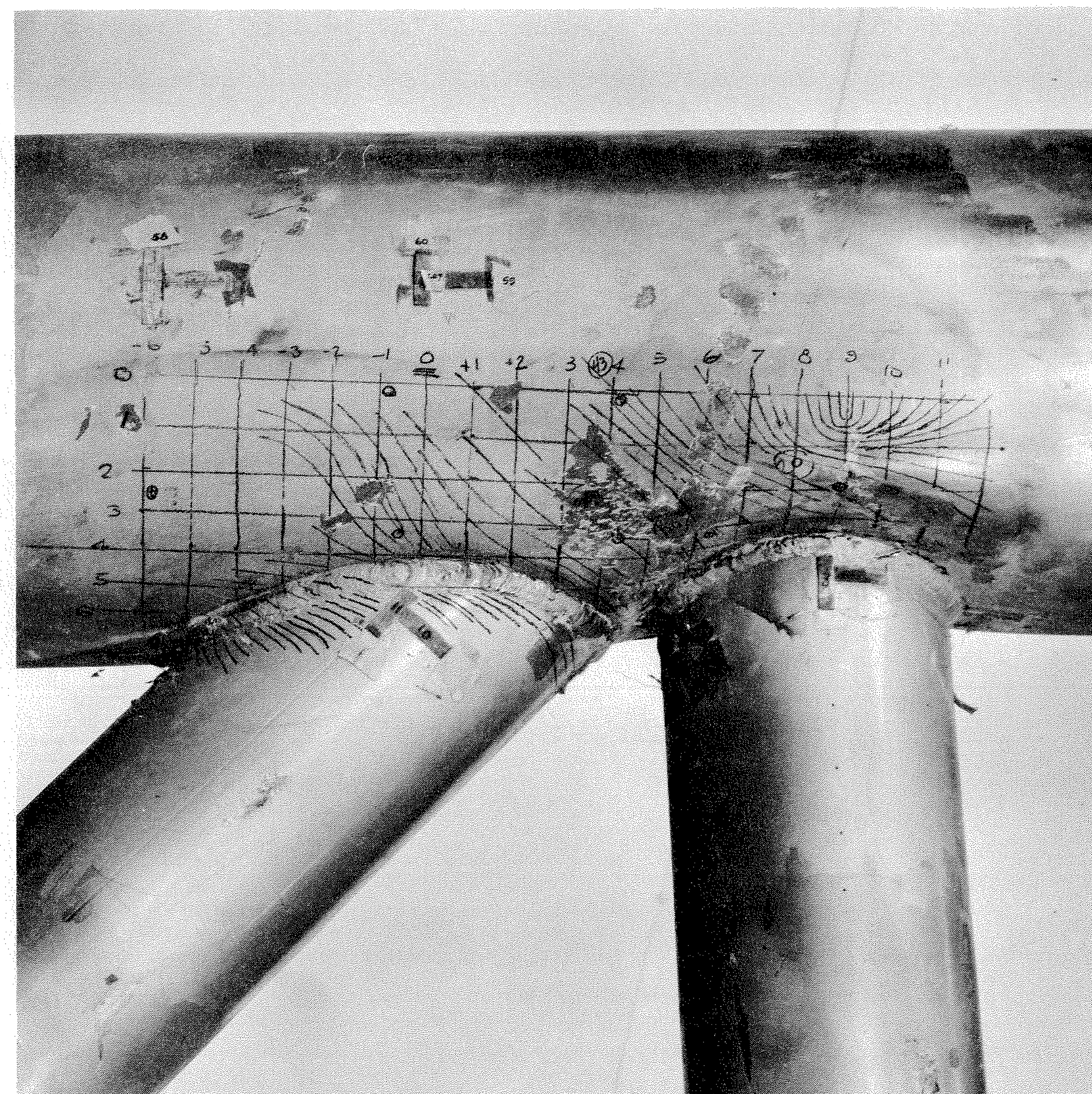

MARKED STRESS-COAT CRACKS FOR POSITIVE-ECCENTRICITY JOINT

FIG. 21

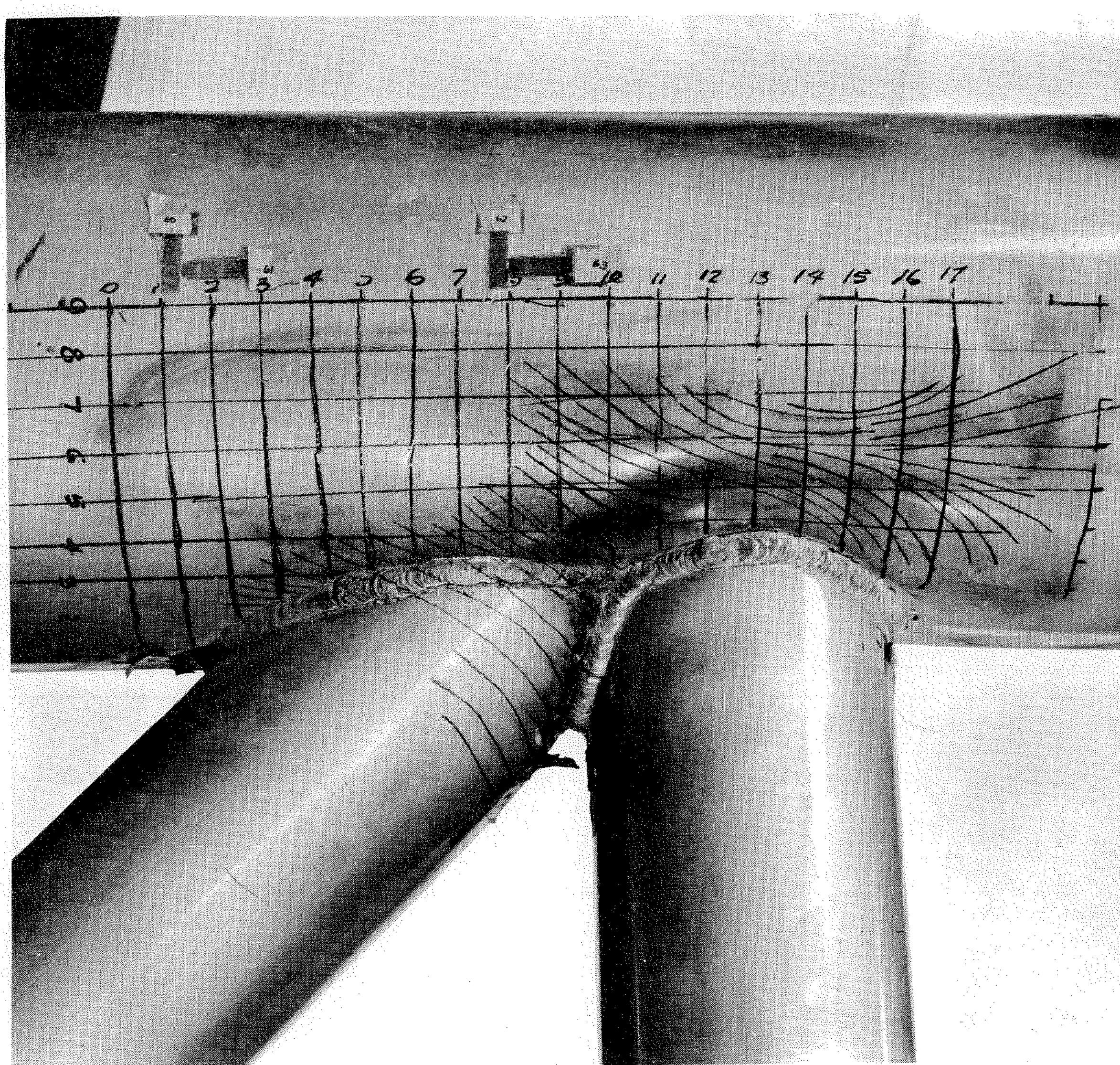

MARKED STRESS-COAT CRACKS FOR ZERO-ECCENTRICITY JOINT

FIG. 22

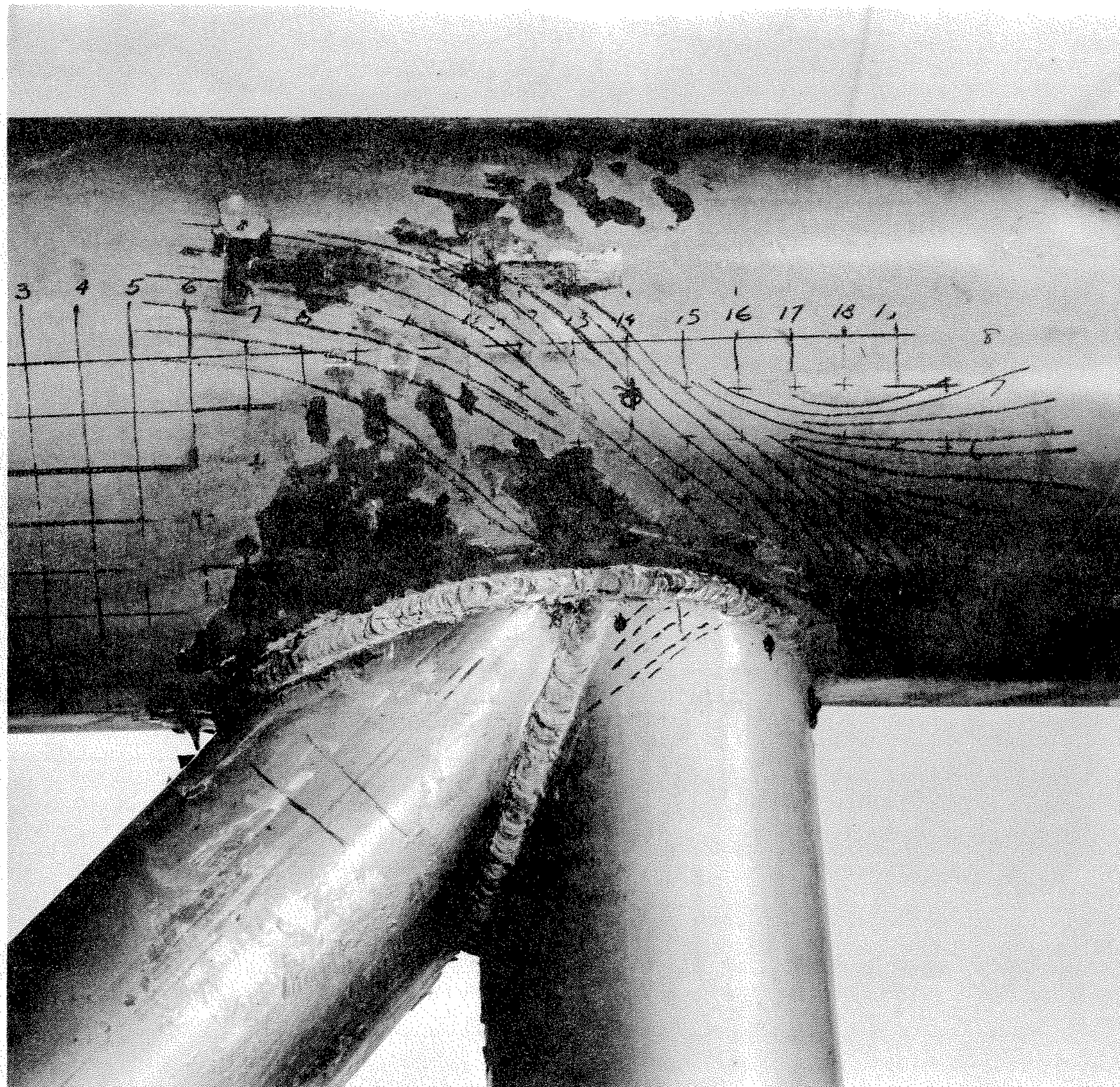

MARKED STRESS-COAT CRACKS FOR NEGATIVE-ECCENTRICITY JOINT

FIG. 23